AOPP, UNIVERSITY OF OXFORD

Sloping Convection: An Investigation into Period-Doubling Bifurcations and Inertia-Gravity Waves in a Baroclinic Annulus

First Year DPhil Report

Samuel David Marshall

Lincoln College

Supervisor: Professor Peter Read

28/8/2010

Word Count: 14,459

Abstract

This report documents the first year of work for this thesis, in which a differentially-heated annulus is used to investigate sloping convection. To this end two studies were made, searching for evidence of temporal period-doubling bifurcations and inertia-gravity waves in a laboratory annulus. Each study was motivated by a numerical investigation that had discovered the phenomena in computational annuli models. The experiments were conducted using an existing apparatus, modified for these studies, the construction and design of which are provided and explained. For the first study, due to issues visualising their location in parameter space, the bifurcations were not observed at this time. However, evidence of spatial period-doubling was uncovered instead. In the second study, instability rolls in the thermal boundary layer, caused by inertia-gravity waves, were recorded. Preliminary observations were made, noting that the rolls grew with increased rotational forcing and occurring at a greater depth with increased thermal forcing. The results of these studies provided a greater understanding of the annulus, allowing improvement of the experimental arrangement for future work. Subsequent years of this thesis will focus on the issue of topography, discussed in this report via a review of the most notable outstanding questions found in the literature. It was decided that the topographic investigation will examine the viability of less-idealised topography, in particular by investigating the effect of using a superposition of wavenumbers rather than a simple sinusoid.

Table of Contents

Chapter 1

Introduction

Sloping convection – and the accurate comprehension of its implications – are arguably the most important aspect of atmospheric circulation, whether discussing the Earth, other planets within the Solar System, or even exoplanets still to be discovered. Also known as baroclinic instability, sloping convection can occur when a thermally-forced zonal flow causes a shear in the density stratification, as in Figure 1.1.

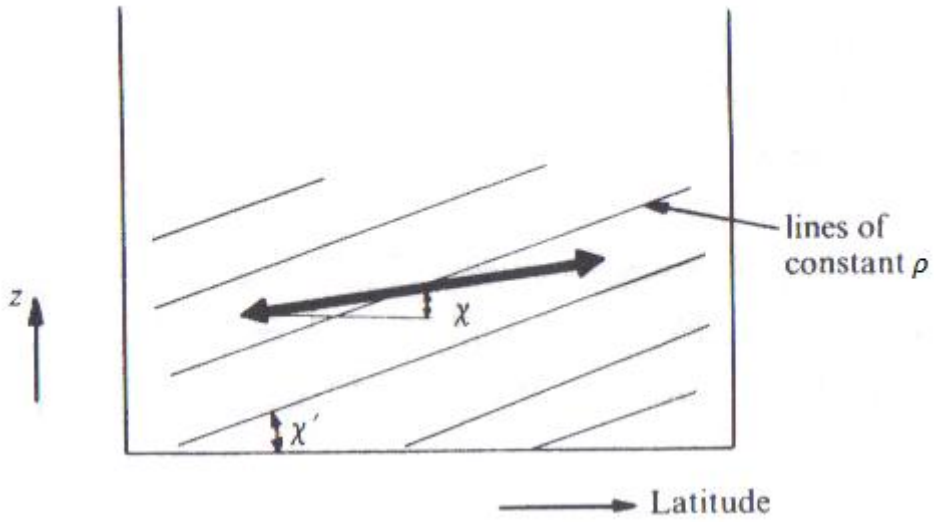

Figure 1.1: Illustration of sloping convection, where χ is the slope between air parcels and χ' is the slope of the density surfaces [adapted from Houghton (2002)]

If $\chi < \chi'$, this shear leads to an increase in potential energy, due to the interchange of the air parcels between surfaces of different densities, in turn providing kinetic energy into the system and hence producing instabilities. A more detailed account of this process can be found in Andrews (2000).

The effects of sloping convection on the atmosphere are many and various. For example, Houghton (2002) notes that, outside of the Hadley Cell, sloping convection is the dominant method of heat transport in the atmosphere, and, according to Hide, Lewis and Read (1994), it is also a probable mechanism for the generation of such famous and long-lasting features as the Jovian Great Red Spot.

In the laboratory, sloping convection can be replicated using a piece of equipment known as a differentially-heated rotating annulus. As such, this thesis will utilise this apparatus to study the various impacts that sloped convection of the fluid has on the patterns governing atmospheric circulation, with special focus on the differences between quasi-geostrophic and ageostrophic effects.

1.1 The Annulus

The rotating annulus is the standard for laboratory studies of the atmosphere, especially with topography. Differentially-heated annuli, such as those in Leach (1981), Li, Kung and Pfeffer (1986) and Risch (1999), are cylinders full of fluid on a rotating turntable that contain a second central cylinder which can be cooled, whilst the outer cylinder can be heated – this temperature difference is what drives the flow. In this way, the annulus becomes a simple simulation of the Earth's (or another planet's) atmosphere, as seen from directly above the poles, with the cool middle analogous to the pole, and the heated outer edge analogous to the equator. More specific detail will be provided in a later section.

Annuli have their origin in the early 'dishpan' experiments of the 1800s, most notably that of Vettin (1857), who used a container of ice to cool the center of the fluid. Unfortunately, only Vettin was able to see the importance of this model of the atmosphere, and the development of the experiments stalled. The next time annuli would occur in major literature would be almost one hundred years later, in Hide (1953). Interestingly, these annuli, despite essentially being in their modern form (with only minor differences in materials and structure), were designed to study the thermal convection in the Earth's core. However, Hide did note the possible application to atmospheric circulation. By the time of Hide (1958), interest in atmospheric circulation had overtaken that of the Earth's core and the first modern investigation with an annulus led to the discovery of vacillation and the different flow regimes of the jet stream (including a detailed images of wavenumber-2, wavenumber-3 and wavenumber-4 regimes, described in the next section). Several years later, Hide and Mason (1975) produced the seminal work on annuli, and the basis for most modern experiments. The authors investigated the effects of increasing the rotation rate and thermal forcing on the flow, charting the transition from wavenumber-1, through wavenumber-2, wavenumber-3 and wavenumber-5, up to the chaotic/irregular regimes. As will be seen, the experimental arrangement of this thesis owes a lot to these studies.

1.2 Sloped Convection in the Annulus

The temperature difference of the differentially-heated annulus generates a radial flow (analogous to the atmosphere's meridional flow) that acts to create a baroclinic flow profile. This can be observed by taking temperature readings of the fluid, as illustrated in Figure 1.2, which shows a temperature stratification that represents the sloping density surfaces.

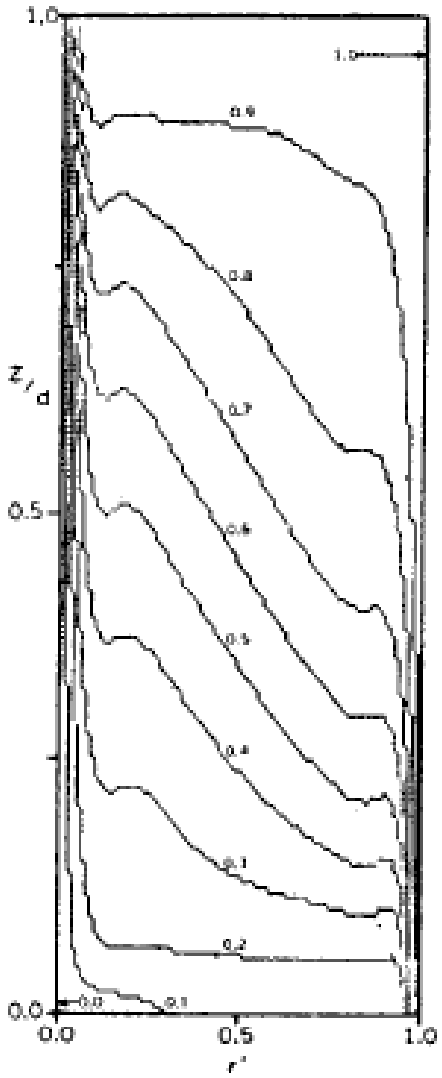

Figure 1.2: Cut-away of computational annulus showing normalised temperature contours with respect to height/depth (y-axis) and radial distance (x-axis) [from Williams (1967)]

Hence, sloping convection can be simulated in the annulus, along with its dynamical effects on the flow. These effects can be split into two types: quasi-geostrophic and ageostrophic.

The quasi-geostrophic approximation assumes that the Rossby Number (the ratio of inertial acceleration to Coriolis acceleration, explained in the next chapter) is small but non-negligible, allowing derivation of the quasi-geostrophic potential vorticity which, in terms of the streamfunction ψ, can be written in the form:

$$q = f_0 + \beta \cdot y + \frac{d^2\psi}{dx^2} + \frac{d^2\psi}{dy^2} + \frac{d}{dz}\left(\frac{{f_0}^2}{N^2}\frac{d\psi}{dz}\right) \tag{1.1}$$

where x, y and z are the zonal, meridional and vertical directions respectively, β and f_0 (the planetary vorticity, which can be omitted due to being constant) are from the beta-plane approximation to the Coriolis parameter $f \approx f_0 + \beta \cdot y$ and N is the buoyancy frequency. This is a very useful result, allowing a single unknown, q, to describe the entire motion of the system. As such, quasi-geostrophic models are very common, often employed even when the approximation starts to break down, for instance when topography becomes large enough.

Quasi-geostrophic dynamics are low-order phenomena, achievable by simple numerical models with only a small number of modes. Ageostrophic dynamics, on the other hand, require either high-resolution computational models or laboratory studies to be observed. In the next two sections, the most important occurrences of both will be briefly introduced and discussed.

1.2.1 Quasi-Geostrophic Dynamics

The most important low-order effect of sloping convection in an annulus is the advent of baroclinic waves. At low rotation rates, flow structure is uniform in the azimuthal direction[1]. Hide and Mason (1975) refer to this region as 'axisymmetric'. When the rotation rate surpasses a certain critical value, however, the flow becomes 'non-axisymmetric' and azimuthal variation is introduced in the form of eddies. The number of eddies that occur increases with increased rotation (and/or thermal forcing) until a second critical value is reached whereupon the structure becomes dominated by chaos. These eddies are baroclinic waves, and are illustrated in Figure 1.3.

[1] Andrews (2000) notes the similarity to the Hadley Cell circulation.

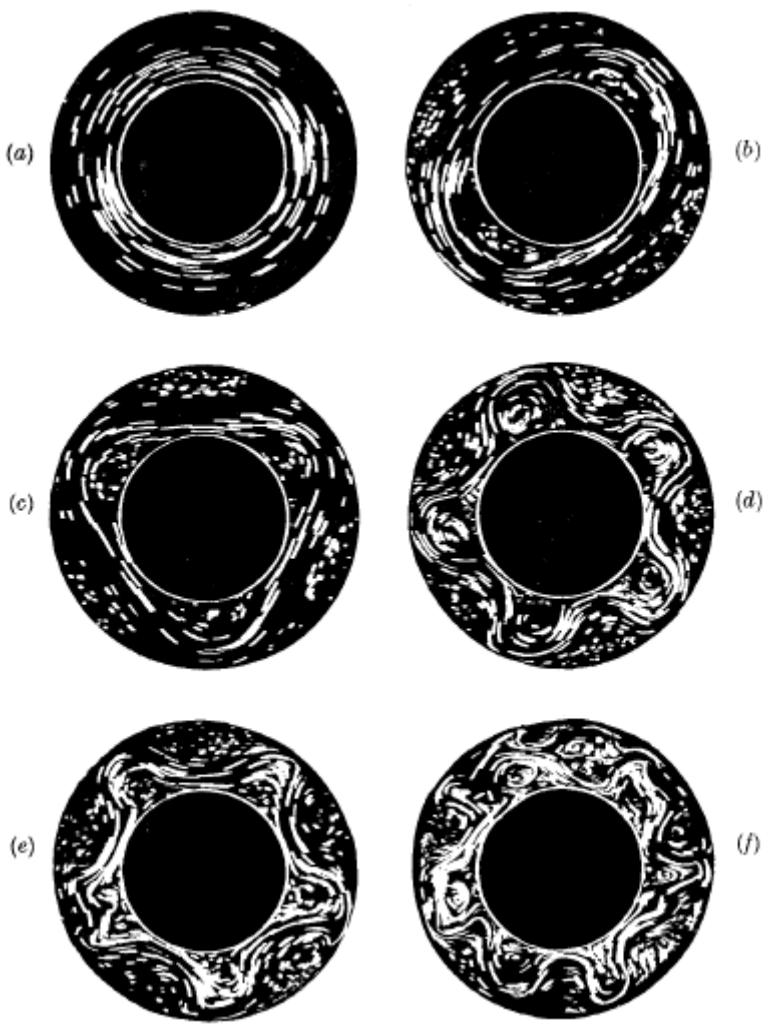

Figure 1.3: Streakline images illustrating how the flow structure develops as rotation rate increases - a.) $\Omega = 0.41$ rads^{-1}, b.) $\Omega = 1.07$ rads^{-1} c.) $\Omega = 1.21$ rads^{-1} d.) $\Omega = 3.22$ rads^{-1} e.) $\Omega = 3.91$ rads^{-1} f.) $\Omega = 6.4$ rads^{-1} [from Hide and Mason (1975)]

Each flow structure is named after the 'period' of the waves, with (b) referred to as wavenumber-2, (c) as wavenumber-3, (d) as wavenumber-5, and so-on. Furthermore, the waves can be either stationary or drifting, depending on whether they oscillate at the same rate as the annulus or not, and either vacillating or steady, depending on whether the eddies maintain a constant size and shape or not. Amplitude vacillation is where the eddies grow or shrink in the radial direction over time, and structural vacillation (which occurs with more intense forcing) is where the eddies change in appearance, for example becoming unevenly spaced around the annulus. These terms will become important in describing the results of this thesis' experiments.

The transitions between baroclinic wave regimes lead to another aspect of sloping convection: temporal period-doubling amplitude vacillation. This phenomenon was investigated by Young and Read (2008), in a computational study of a differentially-heated annulus. Period-doubling amplitude vacillation has been noted in other annulus studies, such as in Hart (1985) where the forcing is generated by differential rotation, but Young and Read present the first case of the regime occurring in a purely thermal forced annulus. As the name suggests, the regime was defined as a wavenumber-2 amplitude vacillation that undergoes period-doubling bifurcations until chaos is reached. The bifurcations were observed as multiple or aperiodic loops in delay coordinate reconstructions, with the notation of 2AV-d1 for a single loop (this can be differentiated from a normal wavenumber-2 amplitude vacillation, referred to as 2AV, by the width of the attractor), up to 2AV-dh for higher order aperiodic states.

The authors suggest the possibility of a bifurcation sequence (shown in Figure 1.4), where, by increasing the Taylor Number, the flow gains periodicity at state 2AV-d1, bifurcates to 2AV-d2, continues bifurcating to the chaotic state 2AV-dh (A), oscillates between 2AV-d3 and 2AV-dh (B), settles on 2AV-d3 (C), returns to 2AV-d1 (D), before finally losing periodicity again.

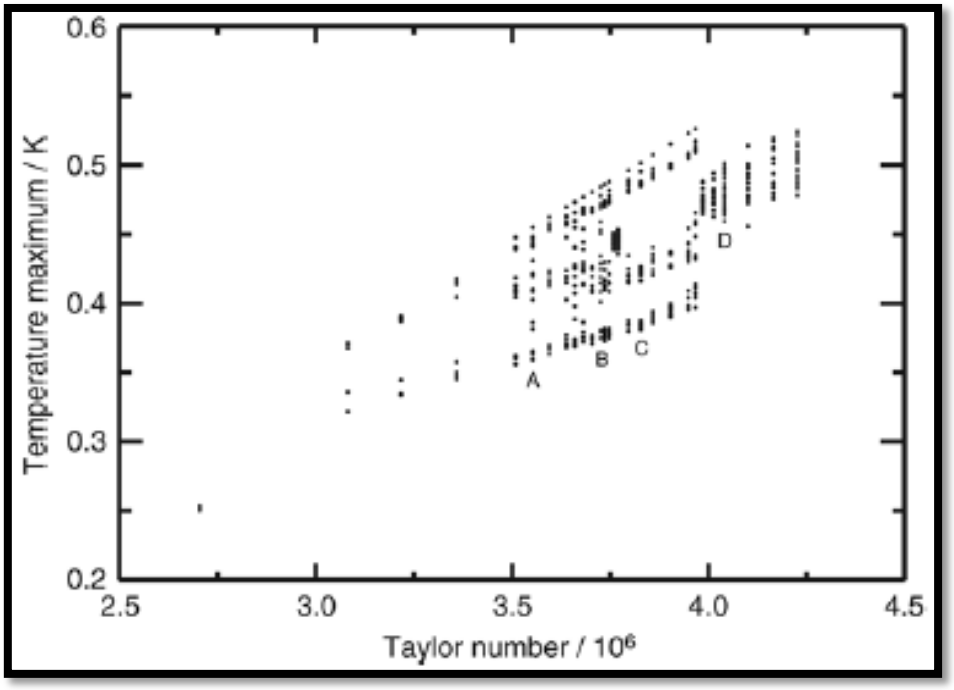

Figure 1.4: Possible bifurcation sequence of wavenumber-2 regime [from Young and Read (2008)]

As these bifurcations have not yet been observed in a physical differentially-heated annulus, part of the first year of this thesis will consist of a laboratory study, attempting to replicate the proposed period-doubling sequence. The objective of the study will be to perform experiments in the same parameter space as Young and Read (2008), verifying the existence of the bifurcations by creating delay coordinate reconstructions from velocity data. From that point, further investigations can be made, examining the links between period-doubling and such areas as Rayleigh-Bénard convection and turbulence (as discussed in Gollub and Benson (1980), for example).

A secondary objective of this study will be to gain a working knowledge of the experimental rig. By using an unmodified rig to verify the findings of a recent numerical investigation, the results gathered should improve the approach for the subsequent years of research. Hence, after the conclusion of the study, it is hoped that the understanding of the annulus obtained will clarify how best to re-design the equipment arrangement for optimal performance.

1.2.2 Ageostrophic Dynamics

Inertia-gravity waves are amongst the most notable examples of the ageostrophic effects of sloping convection. They are ageostrophic as they form within the thermal boundary layer of the annulus, which cannot be modelled by quasi-geostrophic theory. Whilst inertia-gravity waves have a shorter period and are less apparent in annulus experiments than baroclinic waves, in the atmosphere they have recently been linked to both the occurrence of turbulence[2] and transitions between wavenumbers[3]. Jacoby et al (2010) also note that the momentum transport they provide is essential to the understanding of the atmospheric circulation. Despite the obvious importance of inertia-gravity waves, their mechanism of generation in the annulus remains unknown.

In the annulus, Jacoby et al conducted a numerical study, finding small-scale "overturning events" in the divergence and temperature fields within the boundary layer at the inner wall. These downwards-propagating features were found to drift in phase azimuthally with the baroclinic waves of the main flow. Due to the periodic nature of these structures, they were named 'instability rolls', pictured in Figure 1.5. The rolls were put forward by Jacoby et al as a possible cause of inertia-gravity waves in the annulus.

[2] By Knox, McCann and Williams (2008).
[3] By Williams, Read and Haine (2003).

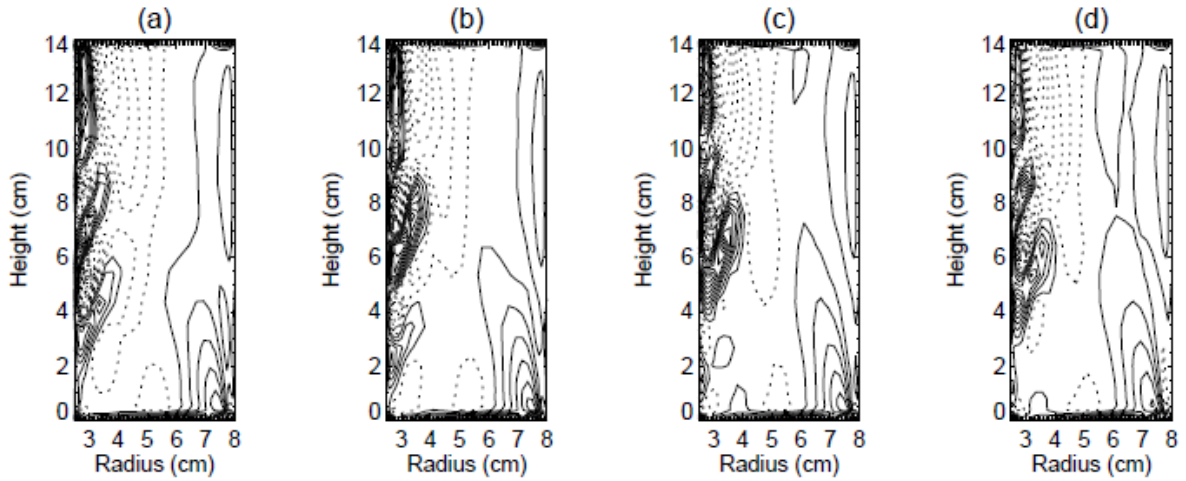

Figure 1.5: Cut-away at fixed azimuth of computational annulus showing divergence field, with the inner wall on the left-hand side. Each image is 12 s apart [from Jacoby et al (2010)]

Due to the difficulty of observing behaviour inside the thermal boundary layer using a physical annulus, few laboratory studies have been conducted into these instabilities. As such, another first-year study in this thesis will be devoted to investigating the evolution of inertia-gravity waves, adapting the apparatus in such a way that the instability rolls can be examined. Once again, the first stage will be a verification of the results of the numerical study, with the second stage being an extended investigation, primarily focussing on the unidentified mechanism of generation.

When topographical features are included in a model, most of the flow dynamics are considered to be ageostrophic. This is due to the quasi-geostrophic approximation starting to break down when topography becomes large enough. Benzi et al (1986) stated that, if there were no topography, the long-term atmospheric circulation would be zonally symmetric (although, short-term asymmetry can be caused by differential heating). Hence, topography must have a spatial symmetry-breaking effect on the zonal flow, which takes the form of stationary topographic waves. These waves[4] are defined as having peaks and troughs that do not move relative to the ground, occurring at locations determined by the shape of the planet's topography. According to Wallace (1983) topographic forcing is dominant at the level of the jetstream, between the middle and upper atmospheres. At sea level, thermal forcing takes over. This is backed up by Held (1983); however he asserts that the effect of topography is still non-negligible at the surface.

[4] Occasionally referred to as quasi-stationary waves, as in Cehelsky and Tung (1987), for example.

Another influence of topography on the atmosphere is the formation of flow regimes, as explained by Charney and DeVore (1979). Topographical forcing can lead to the development of either a 'low index' flow or a 'high index' flow. The former state (also known as 'blocking') is defined as having "a strong wave component and a weaker zonal component locked close to linear resonance"; this locking is caused by the non-linear interactions of the topography with the zonal flow. The latter state (also known as 'zonal' flow) has "a weak wave component and a stronger zonal component much further from linear resonance". Both states are stable (sometimes also referred to as metastable or quasi-stable), giving rise to the concept of multiple equilibria. Transitions between the two states are forced by baroclinic instabilities of the topographic waves.

As topography is so important to atmospheric circulation (with the above only giving a few effects), a topographic study will form the major part of this thesis, with an experimental investigation beginning in the second year. More impacts of topography will be discussed in Chapter 5, along with unresolved questions found from a review of the literature on the topic. It is the answers to these questions that will determine the course of the topographic study, as well as the precise nature of the experiments to be carried out.

1.3 Summary

The format that this report will take is as follows. Firstly, Chapter 2 will be a detailed account of the experimental apparatus that this project will utilise, including the methodology that will be employed and explanations of the experiments to be carried out in the first year of study. The chapter will also contain a short explanation of some of the key dimensionless numbers needed to describe the parameter space. Next, Chapter 3 will provide the results of these experiments, and contain initial observations made. This will be followed by a discussion, Chapter 4, examining the progress of the first year of study and suggesting outstanding issues for later investigation. Chapter 5 will then move on to the planned research on topographic effects to be undertaken in the second and third years of the thesis, describing what unresolved questions about the effects of topography on the atmospheric circulation remain to be investigated, what laboratory work has already been carried out on the subject and how the current apparatus can be altered to investigate these effects. Chapter 6 will consolidate all the outstanding issues from the preliminary conclusions and the plan for adapting the annulus for topographic investigation in order to create an outline for the aims and objectives for the next two years of the thesis. In addition, a timeline of work until the end of the project will be established and justified. Lastly, Chapter 7 gives a list of the various references used to assemble this report.

Chapter 2

Experimental Arrangement

This chapter will first explain the apparatus available for this project's investigation, split up into the experimental equipment itself and all the hardware and software needed to actually generate results. Descriptions of the both the basic arrangement used to investigate the bifurcation phenomena and the slightly altered arrangement used to investigate inertia-gravity waves will be given. The next section will detail the process of how everything was put together, and the final section will describe how the equipment will be employed to achieve meaningful solutions to the problems posed in the previous chapter. Firstly, however, a brief introduction to some of the more relevant dimensionless numbers will be provided, in order to give context to the parameter space under investigation.

2.1 Non-dimensional Numbers

Whilst the flow of the atmospheric circulation is extremely complicated, for typical annuli experiments (and computational annulus models) the entire system can be reduced to two dimensionless numbers which fully describe parameter space. Firstly, the Taylor Number is defined as:

$$\mathcal{T} = \left(\frac{f \cdot L^2}{\nu}\right)^2 \tag{2.1}$$

where L is the characteristic length scale and ν is the kinematic viscosity. The Coriolis Parameter, f, also known as the Coriolis Frequency, describes the effect of the planetary rotation (ω) depending on latitude (φ) and is found using the equation:

$$f = 2\omega \cdot \sin(\varphi) \tag{2.2}$$

For an annulus experiment, φ is taken to be 90°, and the Taylor Number can be adapted to the form:

$$\mathcal{T} = \frac{4\Omega^2 (b-a)^5}{\nu^2 \cdot d} \tag{2.3}$$

where a is the inner radius, b is the outer radius and d is the height of the annulus and Ω is the rate of rotation of the fluid. Roughly, the Taylor Number gives the ratio of the Coriolis forces (the

numerator) to the viscous forces (the denominator) acting upon a fluid. A large value implies a less stable flow, with circulation tending toward higher dominant wavenumbers and the irregular regime.

Secondly, the Rossby Number is defined as:

$$\theta = \frac{U}{f \cdot L} \tag{2.4}$$

where U is the characteristic velocity scale of the fluid. For an annulus experiment, this can be adapted into the Thermal Rossby Number (sometimes also known as the Hide Number, hereafter simply 'the Rossby Number') which takes the form:

$$\theta = \frac{\alpha \cdot g \cdot d \cdot \Delta T}{\Omega^2 (b-a)^2} \tag{2.5}$$

where α is the thermal expansion coefficient, g is the gravitational acceleration and ΔT is the temperature difference. Roughly, the Rossby Number gives the ratio of the inertial forces (the numerator) to the Coriolis forces (the denominator) acting upon a fluid. At large values the geostrophic approximation (explained in the next chapter) begins to break down, leading to Houghton (2002) to refer to the Rossby Number as a "measure of the validity of the geostrophic approximation".

As most of the quantities are assumed (or fixed) to be constant, the Taylor Number can be simplified to being proportional to Ω^2, and the Rossby Number can be simplified to being proportional to $\frac{\Delta T}{\Omega^2}$. For an annulus experiment (or similar) the rotation rate and the temperature difference are the main sources of control, hence, these two dimensionless numbers can be taken to fully describe the parameter space that the experiments take place within, as noted by Hide and Mason (1975) in their pioneering study of the annulus.

For the study of inertia-gravity waves, a third dimensionless number becomes important – the Prandtl Number, defined as:

$$Pr = \frac{\nu}{\kappa} \tag{2.6}$$

where κ is the thermal diffusivity. The Prandtl Number gives the ratio of the viscous diffusion (the numerator) to the thermal diffusion (the denominator) acting upon a fluid. White (2008) gives the alternate definition of the ratio between dissipation and conduction. In annulus experiments, the Prandtl Number is dependent on the working fluid employed. There exists a critical value of roughly 12 (Randriamampianina, private communication) where the inertia-gravity waves change from being stationary waves to drifting waves. A further review of the importance of the Prandtl Number can be found in Fein and Pfeffer (1976) or Randriamampianina et al (2006).

2.2 Equipment Description – Bifurcation Study

Accounts of the annulus in question can be found in the theses of two of its previous users - Risch (1999) and Wordsworth (2008). The latter is more helpful, as it is more recent (thus the electronics are more up-to-date) and Wordworth made several changes to the annulus, replacing the O-ring seals and decreasing the radius of the inner cylinder to permit higher Taylor Numbers to be reached. Figure 2.1 provides two labelled photographs of the annulus, illustrating the apparatus described in this chapter.

a.)

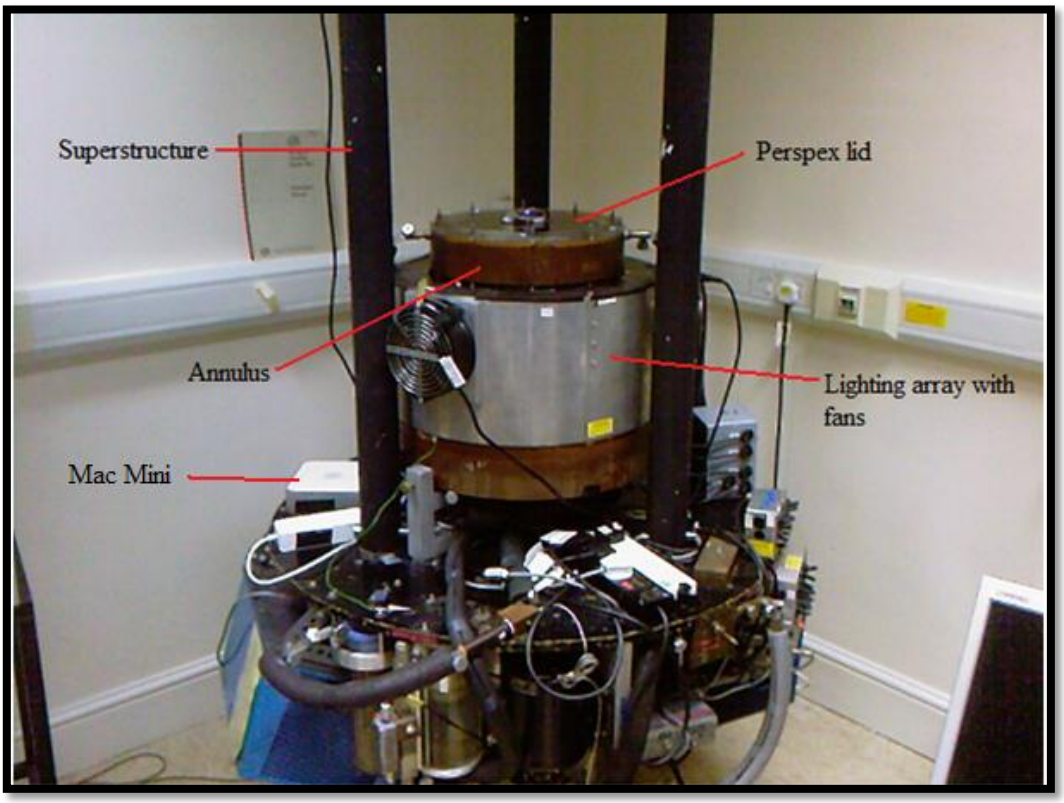

b.)

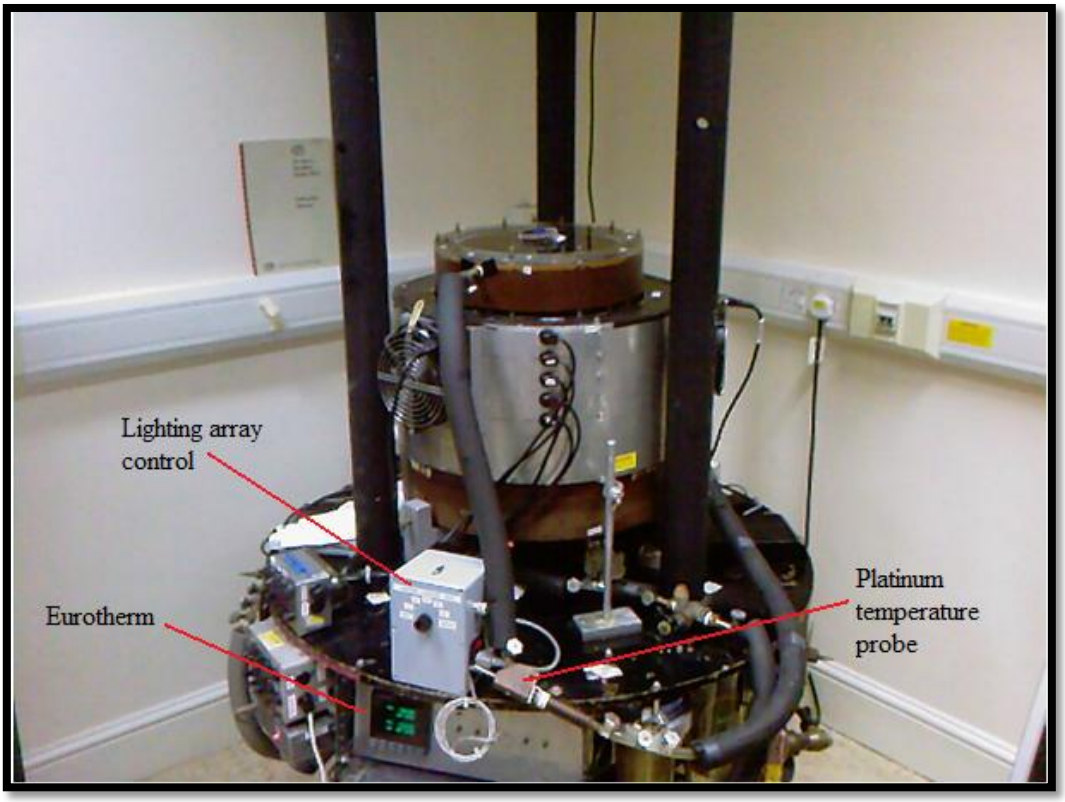

Figure 2.1: Annotated photographs of the annulus from two different sides, with apparatus arranged for the bifurcation study.

As explained in the previous chapter, an annulus functions by setting up a temperature difference between the heated outer edge and the cooled inner cylinder. This is achieved via two flows of water that each travel through a separate circuit containing a pump, a refrigerator, a heater, a filter and a platinum temperature probe. A feedback system between the probes and a Eurotherm 900 EPC Temperature Controller manipulates the temperature of the water entering the outer edge or the inner cylinder to any specified value. The entire organisation is shown in Figure 2.2.

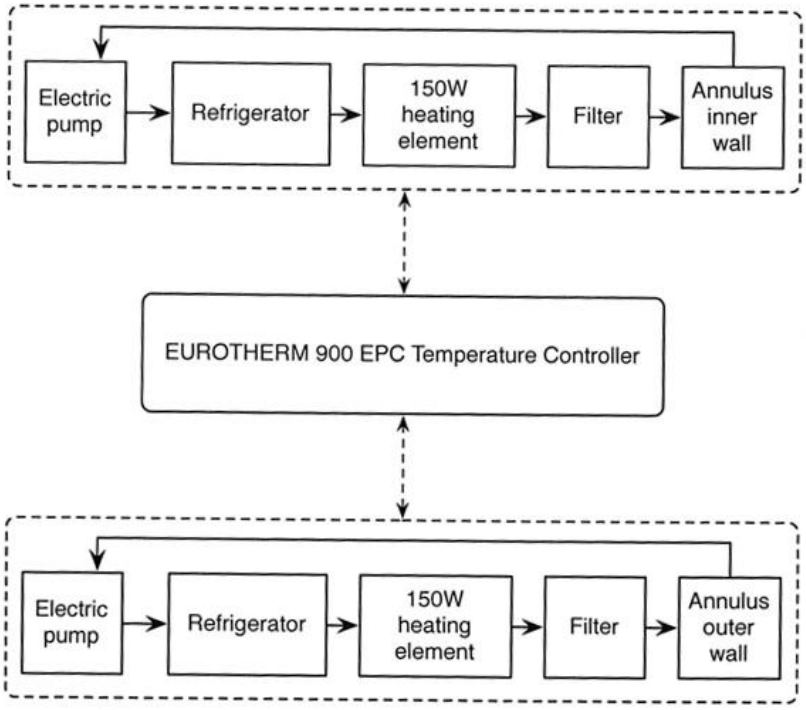

Figure 2.2: Block diagram of heating and cooling flow circuits and feedback system [from Wordsworth (2008)]

The annulus itself is made of Bear grade Tufnol, a resin-bonded multi-layer fabric, and brass, both materials chosen for their thermal properties. The rigid lid is kept in contact with the working fluid and is made of Perspex, for its transparency. The working fluid is a mixture of water and glycerol, made up so that its density is 1.044 kgm^{-3} (the exact ratio of compounds was deemed unimportant, but will be roughly 17% glycerol). This density allows 350-500 μm pliolite tracer particles to be neutrally buoyant. It was decided that the value of $1.66x10^{-6}$ m^2s^{-1} for kinematic viscosity used in Young and Read (2008)[5] was inaccurate. Hence, a sample of working fluid was examined in a viscometer, giving a new result of $1.58x10^{-6}$ m^2s^{-1}. A solution known as Sanosil S006 was added to the fluid to prevent mould growth. The lid and the inside of the annulus were also treated with this solution. An array of thirty 50 W halogen lamps over five layers surrounds the annulus, allowing light to pass through transparent slits at those layers. This is illustrated by Figure 2.3.

[5] Taken initially from Hignett et al (1985).

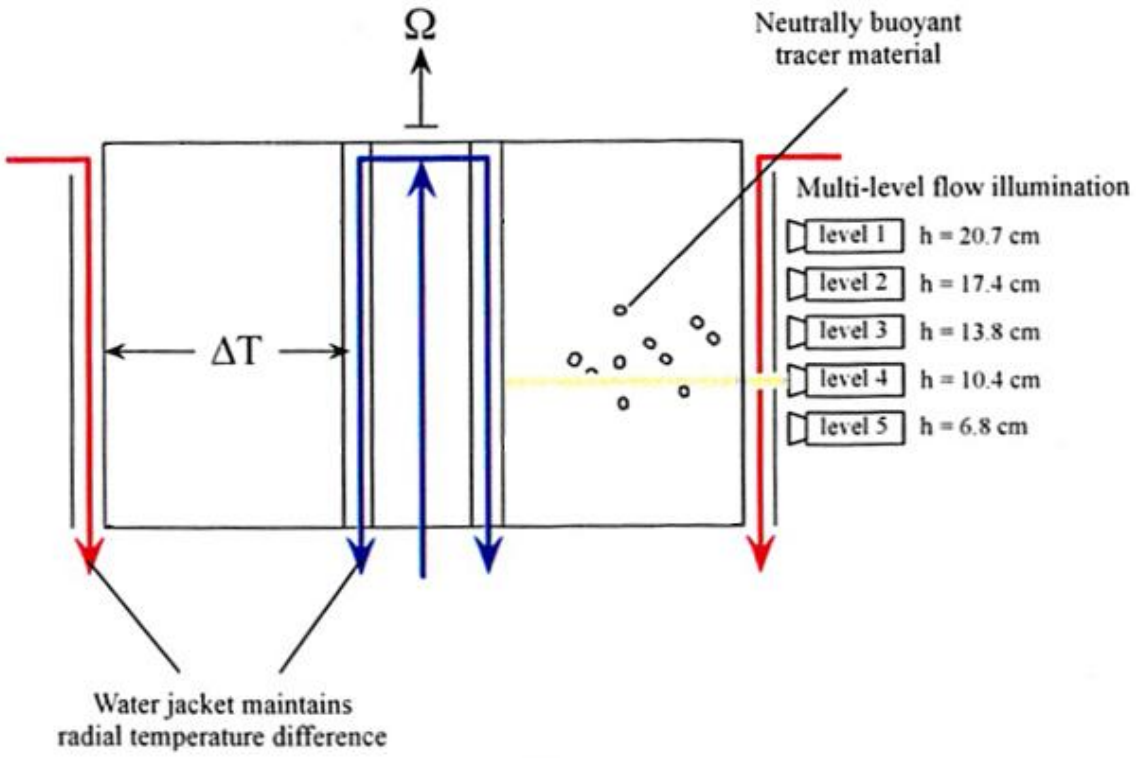

Figure 2.3: Schematic of the lighting array and heating system in side view [adapted from Wordsworth (2008)]

Due to the nature of the halogen lamps, which are very prone to overheating and thus also causing an additional heat source on the outer edge, three large electric fans were attached to the lighting array. An electronic control box controls which of the five layers is illuminated at a time, with an option for an automatic shift between them at a variable rate. A camera is mounted above the annulus on a tripod-shaped superstructure, with a cone blocking all outside light between it and the Perspex lid. With this arrangement, the camera can see the motion of the tracer particles, and thus the flow structure, at any one of the five levels in Figure 2.3. By switching quickly between the layers, the vertical structure can also be resolved.

The annulus to be used is a larger model than the standard, as it was designed for use at high Taylor Numbers. Its dimensions, as well as several other relevant experimental parameters, are given in Table 2.1.

Radius of Inner Cylinder	a	4.5 cm
Radius of Outer Cylinder	b	14.3 cm
Depth of Annulus	d	26.5 cm
Kinematic Viscosity of Water	ν_w	$1.004x10^{-6}$ m^2s^{-1}
Thermal Expansion Coefficient of Water	α_w	$2.07x10^{-4}$ K^{-1}
Density of Water-Glycerol Mixture	ρ_g	1.044 kgm^{-3}
Kinematic Viscosity of Water-Glycerol Mixture	ν_g	$1.58x10^{-6}$ m^2s^{-1}
Thermal Expansion Coefficient of Water-Glycerol Mixture	α_g	$3.16x10^{-4}$ K^{-1}

Table 2.1: Important experimental parameters

2.2.1 Data Acquisition

In deference to previous set-ups, a Firewire (type: DFK 31BF03) camera was selected for taking visual results, due to its high picture quality and supposed simplicity of connection with a Mac Mini computer. The Mac Mini, a recent model, is small and light enough to be mounted to the rotating frame, and saved the images and movies to a 500 Gb Seagate Hard Drive. A Local Area Network (LAN) was set up to allow it to communicate with a second computer in the laboratory frame. This stationary computer is known as the 'base station'. In addition to this digital signal, an analogue signal was also taken from the camera via a slip-ring to a specialised console (a PC and several monitors attached to a SVHS video recorder). It was hoped that both signals could be achieved simultaneously thanks to a Canopus ADVC 110 Analogue/Digital Converter attached to the Mac Mini.

In terms of software, the free TightVNC (Virtual Network Client) package allows the base station to remotely control the Mac Mini, and therefore the camera functions. The specialised console used a program known as Digimage to create streak-line images and movies from the analogue signal. These results give an idea of the type of flow at a given point: which wavenumber most resembles the motion, whether the waves are stationary or drifting and whether any kind of vacillation is observed. However, due to the noise of the signal and the age of the analogue equipment, these results are of no use for further analysis. The digital signal, on the other hand, goes through a slightly more complicated process. It is picked up on the base station by a software program called BTV Pro, which takes movies of the flow in motion and makes hundreds of frame-by-frame images from them. BTV Pro also ensures the gain of the camera is constant, so that each image occurs under the same conditions. These images are then transferred to a MATLAB program called Coriolis, an example of Correlation Image Velocimetry (CIV) – an iterative algorithm that tracks the translation, rotation and shear motion of the tracer particles. From this information, CIV creates a velocity vector field of the flow, with the option of manually removing any false readings. Modal analysis of the vector field should prove extremely important for detailed examination of the fluid structure, including the ability to create delay coordinate reconstructions, for use in the investigation of Young and Read's (2008) bifurcations.

2.3 Inertia-Gravity Wave Study Arrangement

For the study of inertia-gravity waves it was necessary to examine the fluid motion within the thermal boundary layer, hence the experimental arrangement required a few modifications. The most notable of these was an alternative visualisation method, created by removing the tracer particles and injecting a solution of Fluorescein sodium (a luminous green dye) directly into the boundary layer via a needle held very close to the inner wall of the annulus. The amount of dye added was controlled using a remote-operated mechanical syringe pump. To improve the clarity of the images obtained, one half of the inner wall was painted white. The whole arrangement is shown in Figure 2.4.

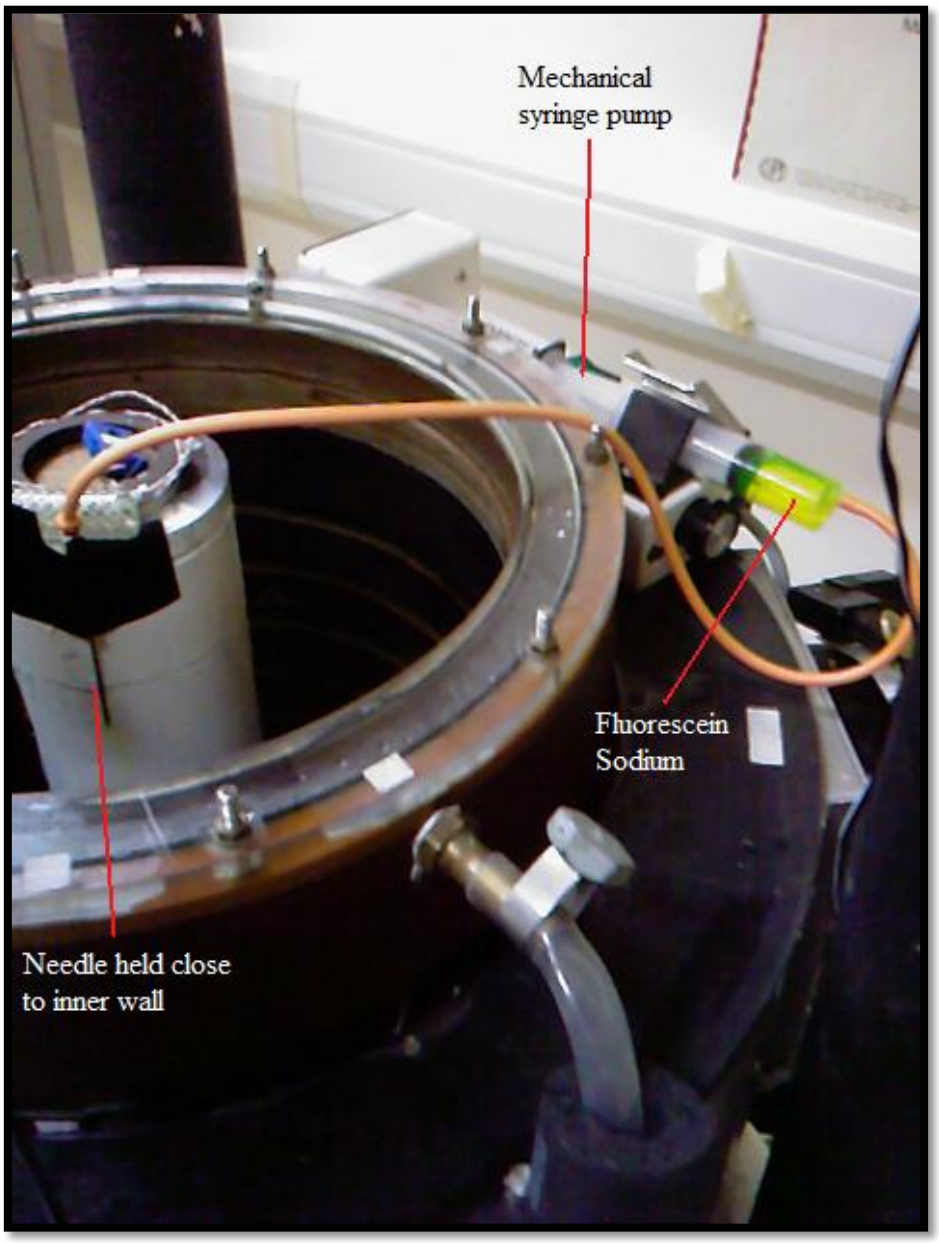

Figure 2.4: Annotated photograph of dye injection system

With the tracer particles replaced with dye, the overhead camera was no longer useful. Hence, a Sony DCR-HC44 MiniDV camcorder was attached to the top of the lighting array, angled so that the full depth of the inner cylinder could be observed. The camcorder was connected to the Mac Mini via a Firewire cable, so the software used was unchanged. Preliminary experiments found that the inside of the annulus was too dark to distinguish the dye, so an additional lamp was fastened to the superstructure. These further modifications are pictured in Figure 2.5.

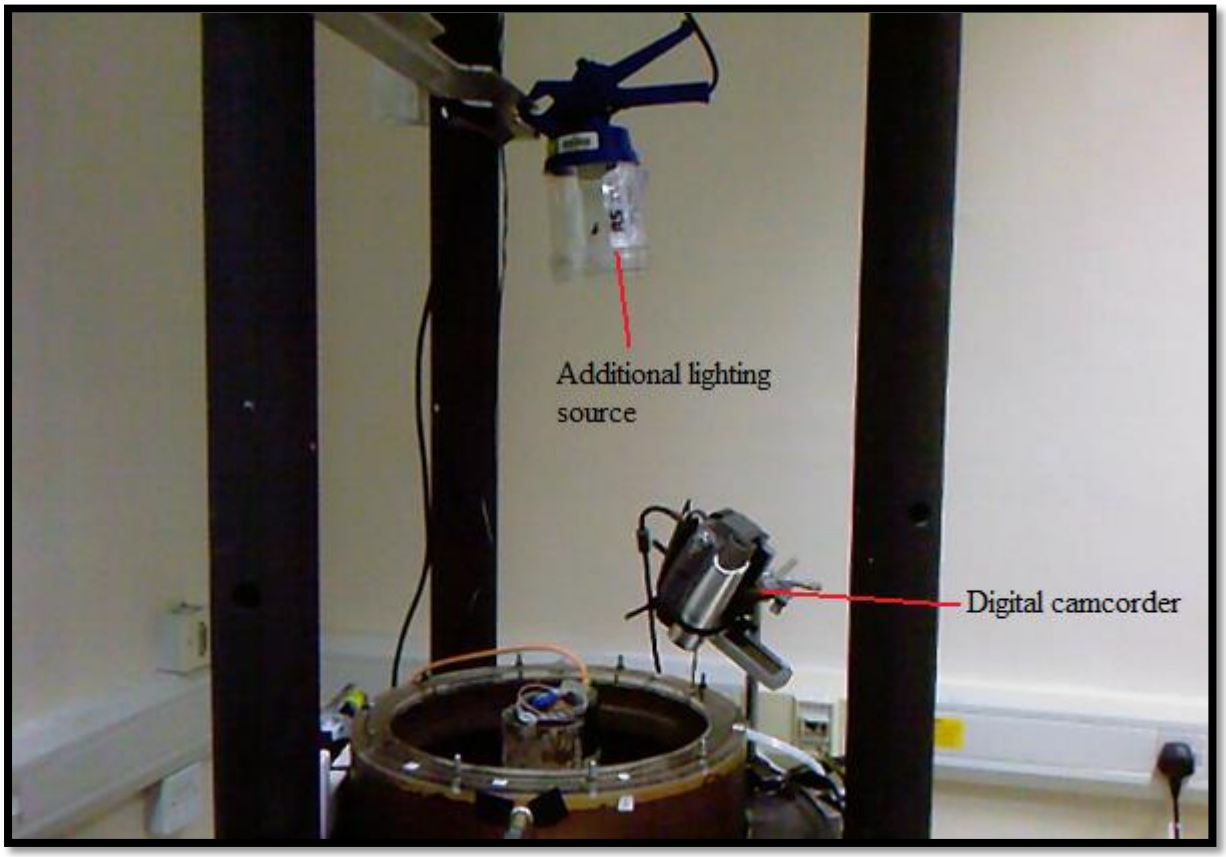

Figure 2.5: Annotated photograph of mounted camcorder and additional lighting

To allow the dye to be injected, these experiments were performed without the Perspex lid. As the instability rolls were expected at a depth of roughly two-thirds from the free surface, and the needle was already partially immersed in the fluid, it was assumed that the effects of contact with the air could be ignored.

As previously mentioned, there is a critical value (at approximately 12) for the Prandtl Number which determines whether stationary or drifting inertia-gravity wave instabilities should occur. Hence, to try and observe both forms of the instabilities, it was decided that two different working fluids would be used: water, with a Prandtl Number of roughly 7, and the usual water-glycerol mixture, with a Prandtl Number of roughly 16.

2.4 Process of Re-building and Issues

When the project began, the apparatus had been taken apart to make space for other experiments. Hence, the major task of the first year of work was to restore the equipment to such a point where experiments could be carried out. Before any of this could begin, however, the turntable was tested for an inherent 'wobble' noted by Wordsworth (2008). A bowl of water was placed in the center of the turntable, to see if any asymmetric ripples could be observed. As none were found, it was decided that the reported vibration must have been due to a section of plumbing rubbing against the structure as it rotated. When the re-build was complete, a second vibration test was carried out, once again finding the 'wobble' to be negligible.

To make sure the annulus was positioned exactly in the center of the turntable, an optical cathetometer (also known as a tracking telescope) was employed. Warping of the wooden annulus base caused a small deviation to the rotation, measured by a Baty Dial Test Indicator to have a maximum of roughly 1.5 mm. As this deviation was confined to the base, not the outer or inner cylinders, this was judged to be negligible.

Once all the components were fixed in the correct location, the process of connecting up the plumbing could begin. All the previous pipes and insulation had been lost or discarded when the apparatus was taken apart, so the entire water system was replaced with new material. During this time various leaks were repaired as well as possible and the impellor for the outer cylinder pump was replaced. The electronics were next to be installed, with the camera, Mac Mini and hard drive attached to the superstructure and all those devices (and the fans, lights etc) were connected to the mains via a slip ring. Lastly, the Firewire camera needed a different attachment to the one used by Wordsworth (2008), so a new aluminium bracket was designed and built. Unfortunately, the Firewire camera and the analogue/digital converter were found to be incompatible so, at this stage, only one of the two signals can be obtained at a time.

2.5 Methodology – Bifurcation Study

Young and Read (2008) highlighted their results at four points of given Taylor and Rossby Numbers, illustrated as A, B, C and D by Figure 2.6. Though it has been noted[6] that transitions will occur in different locations for different annuli, these points should form an excellent place start in the search for the bifurcation sequence.

[6] By Hignett et al (1985), for example.

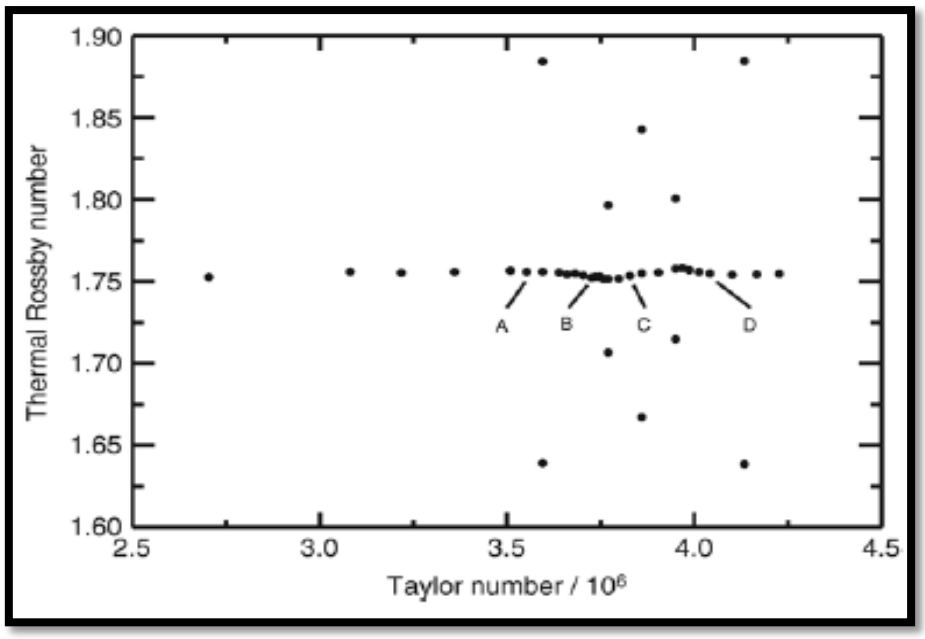

Figure 2.6: Non-dimensional location of the four major results of Young and Read (2008).

This project's annulus is significantly larger than that used by Hignett et al (1985) and Young and Read (2008). This difference is given in Figure 2.7.

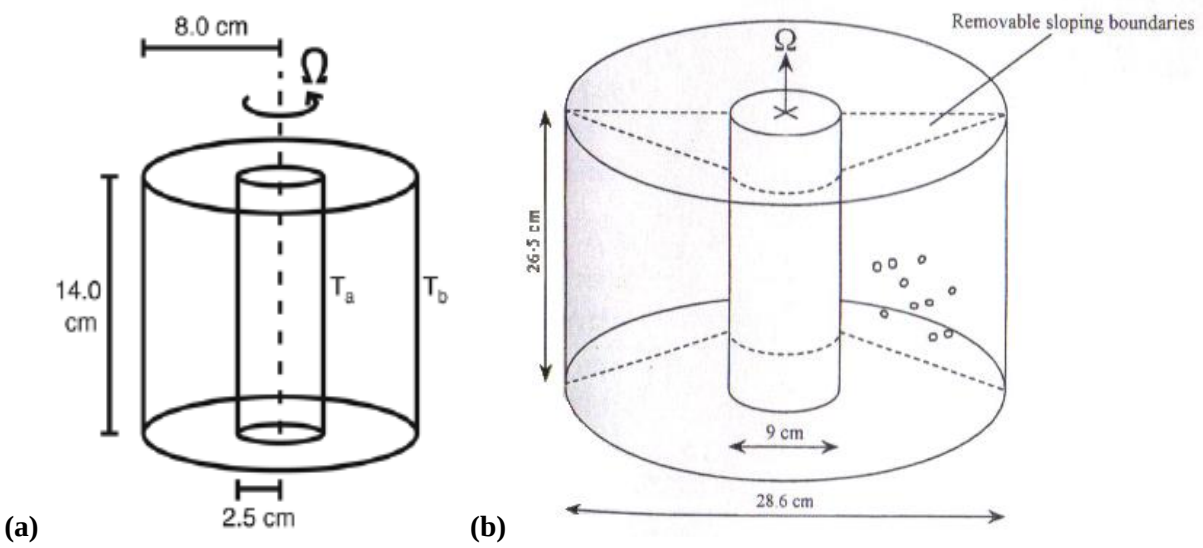

Figure 2.7: Annulus comparison between (a) Young and Read (2008) and (b) the current study [from Wordsworth (2008)]

As the current annulus is larger, *a*, *b* and *d* will all change, altering the Taylor and Rossby Numbers and requiring new values for rotation rates and temperature differences to achieve the same dimensionless numbers, and, in turn, points in parameter space. The calculation of points A, B, C and D from Figure 2.6 with this project's apparatus is shown in Table 2.2.

	A	**B**	**C**	**D**
Taylor Number	3.55×10^6	3.73×10^6	3.83×10^6	4.04×10^6
Rossby Number	*1.756*	*1.752*	*1.754*	*1.755*
Calculated Rotation Rate ($rads^{-1}$)	*0.255*	*0.261*	*0.265*	*0.272*
Calculated Temperature Difference (K)	*1.335*	*1.140*	*1.440*	*1.518*

Table 2.2: Calculation of rotation rates and temperature differences from Young and Read's highlighted results (calculated values to 3 d.p.)

Unfortunately preliminary experiments found that, at these low rotation rates and temperature differences, the evolved wave structure was too weak to maintain the floating tracer, and most of the particles fell to the bottom of the annulus. As such, it was decided to investigate more intense regimes for evidence of period doubling. To this end, and to additionally determine how to achieve the highest quality of results, a great number of different flows were studied. The most important of these are given below:

- An attempt to find the temperature difference at which the particle visualisation technique becomes viable, with differences of 1, 2, 3, 4, 5, 6 and 7 K at a rotation rate of 0.65 $rads^{-1}$.
- High Taylor Number flows at rotation rates of 2.45, 2.75 and 3 $rads^{-1}$ at a temperature difference of 5 K, in order to investigate a chaotic, unstable regime with high forcing.
- Low Taylor Number flows at rotation rates of 0.6, 0.7, 0.8 and 0.9 $rads^{-1}$ at a temperature difference of 3 K, in order to search for bifurcations in an area of moderate forcing.
- A scan[7] with rotation rate increasing at 0.2 $rads^{-1}$ intervals from 1 to 1.6 $rads^{-1}$ at a temperature difference of 3 K, in order to observe the effects of hysteresis.
- A scan with rotation rate decreasing at 0.2 $rads^{-1}$ intervals from 1.6 to 1 $rads^{-1}$ at a temperature difference of 3 K, in order to further observe the effects of hysteresis.

To ensure particle saturation, the annulus was sped up to an arbitrary high rotation rate before being slowed to the relevant speed under examination. The apparatus was then left for one hour to allow the fluid to achieve solid-body rotation and to allow the wave structure to become fully baroclinic. After this point, results were taken over the course of 60 minutes. Due to issues with the illumination from the lighting array, all readings were taken at the brightest height – level 2, at 17.4 cm above the base.

[7] A 'scan' implies that the fluid was not returned to rest between readings.

To begin with, only the analogue signal will be employed, as the real-time streakline images generated by Digimage will allow for easier observation of the bifurcation phenomena. Once evidence of the bifurcations is found, the focus will shift to the digital signal, and the same parameters will be used. In this way, an array of images will be taken via BTV Pro, allowing CIV to create velocity vector diagrams of the flow. Modal analysis of this data can then be used to produce delay coordinate reconstructions, as the shape of the attractor is the best illustration of period doubling.

2.6 Methodology – Inertia-Gravity Wave Study

Whilst the bifurcation study was defined by the attempt to replicate the work of Young and Read (2008), the study of inertia-gravity waves was conducted under the guidance of Peter Read, Wolf-Gerrit Früh and Antony Randriamampianina. The latter suggested a starting place in parameter space of 1.3 $rads^{-1}$ rotation rate and 2 K temperature difference for the water-glycerol mixture experiment, analogous to 1 $rads^{-1}$ rotation rate and 2 K temperature difference for the water experiment. From this point, two investigations could be launched: one into the effects of reducing the rotation rate, the other into the effects of increasing the temperature difference.

For the water experiment this meant that nine separate readings were taken, with three different rotation rates of 0.6, 0.8 and 1 $rads^{-1}$ and three different temperature differences of 2, 5 and 10 K. Due the necessity of having to replace the fluid every few readings because of dye saturation, it was decided that only one of the two investigations would be carried out with the water-glycerol mixture. Preliminary experiments suggested that the reduction in rotation rate would be more fruitful, due to the higher clarity of the images taken at the lowest temperature difference. As such, the water-glycerol mixture experiment took only three readings, with three different rotation rates of 0.9, 1.1 and 1.3 $rads^{-1}$, all at the same temperature difference of 2 K.

In the same way as for the bifurcation study, the annulus was left for one hour after being sped up to the required rotation rate (there was no need for particle saturation) to allow for solid-body rotation and hence a stable thermal boundary layer. Due to the short lifetime of the tracer dye, results were taken over a period of 5 minutes.

Chapter 3

Results

The results of both the bifurcation study and the inertia-gravity wave study are contained within this chapter. More detail on the presented Figures will be explained in the introduction to each section. After each study, a short analysis will be given, describing what is observed and noting any trends discovered. For convenience, a sample regime diagram is provided in Figure 3.1, showing the locations of both the proposed bifurcation sequence and the experiments of this study.

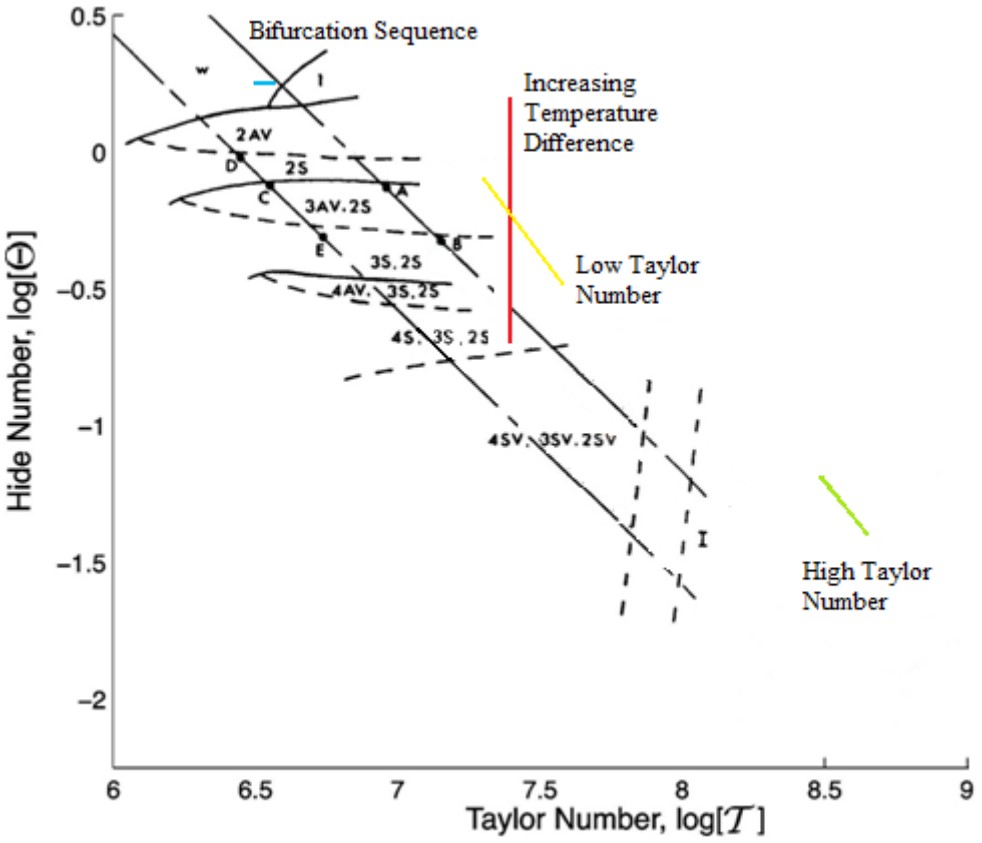

Figure 3.1: Regime diagram with locations of Increasing Temperature Difference (red), Low Taylor Number (yellow) and High Taylor Number (green) experiments, along with the proposed bifurcation sequence (blue). Individual readings are not shown for sake of clarity [originally from Hignett et al (1985); adapted from Wordsworth (2008)]

3.1 Bifurcation Study

For sake of space and clarity, not every result that was taken will be given in this section. In particular the increasing and decreasing scans will be left out completely, as the indications of the phenomena of hysteresis were fairly limited. Streakline images created by Digimage feature a yellow 'head' that shows where the particle being tracked is now, shifting towards a blue 'tail' that shows where the particle has travelled in the last 20 seconds (10 seconds for high Taylor Number flows). For each point in parameter space, three streakline images were taken – the first just after the one hour spin up at 3600 s, the second 30 minutes after that at 5400 s, and the third another 30 minutes after that at 7200 s. Each Figure is marked with this time, as well as the rotation rate, temperature difference, Taylor Number and Rossby Number (dimensionless numbers calculated to 3d.p.).

3.1.1 Increasing Temperature Difference

This run of experiments was carried out to investigate the minimum temperature difference required to allow for viable particle tracking, as well as to study the effects of increasing this parameter on the wave structure.

a.) **b.)** **c.)**

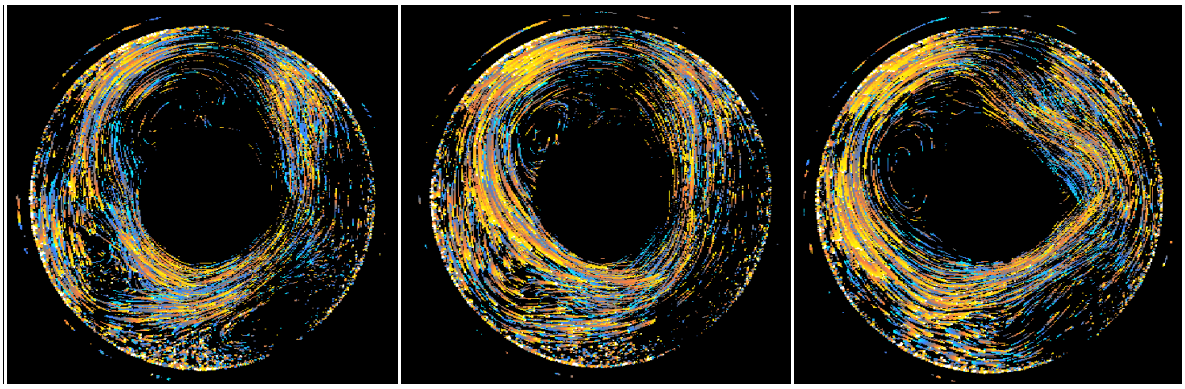

Figure 3.2: $\Omega = 0.65$ *rads*$^{-1}$, $\Delta T = 4K$, $\mathcal{T} = 2.309x10^{7}$, $\theta = 0.810$, *a.)* $t = 3600s$, *b.)* $t = 5400s$, *c.)* $t = 7200s$

a.) **b.)** **c.)**

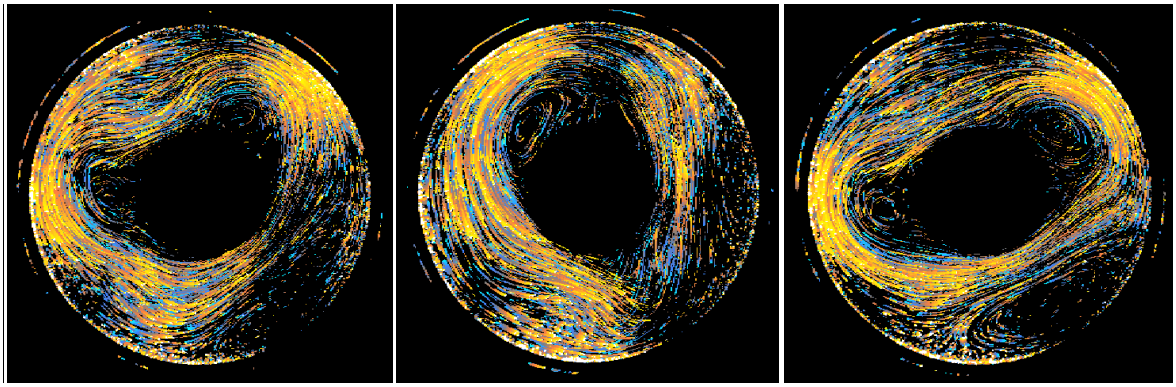

Figure 3.3: $\Omega = 0.65$ *rads*$^{-1}$, $\Delta T = 5K$, $\mathcal{T} = 2.309x10^7$, $\theta = 1.012$, *a.)* $t = 3600s$, *b.)* $t = 5400s$, *c.)* $t = 7200s$

a.) **b.)** **c.)**

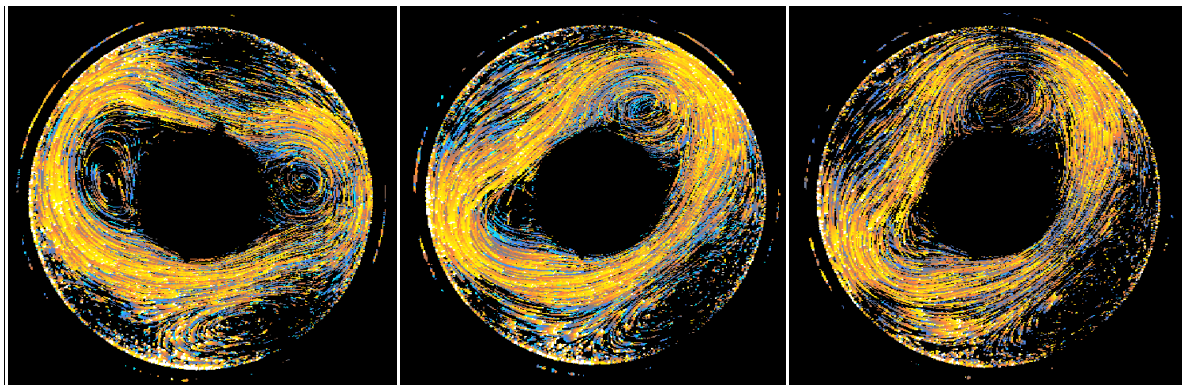

Figure 3.4: $\Omega = 0.65$ *rads*$^{-1}$, $\Delta T = 6K$, $\mathcal{T} = 2.309x10^7$, $\theta = 1.215$, *a.)* $t = 3600s$, *b.)* $t = 5400s$, *c.)* $t = 7200s$

As for the first goal of these experiments, when the temperature difference is 1 K, the particles are too sparse for an accurate reading, appearing almost invisible to the camera. At 2 K, the image is superior, but still loses a lot of information outside of the baroclinic jets (and gets worse with time). Hence, 3 K was the judged to be the first integer temperature difference that permits flow visualisation with the current equipment. The shown results illustrate an increase in flow structure complexity as the temperature difference is raised, with Figure 3.2 illustrating a wavenumber-1, Figure 3.3 appearing to give a transition between wavenumber-1 and wavenumber-2 and Figure 3.4 illustrating wavenumber-2 structure. The latter Figure is also a good example of drifting waves. Figure 3.3 is rather more complicated than it first appears, however, giving images of atypical wavenumber-1 and wavenumber-2 flows, despite its low thermal forcing. Unfortunately, no evidence of period-doubling bifurcations can be observed in any of the results.

3.1.2 High Taylor Number

This run of experiments was carried out within the 'irregular' regime of Figure 3.1, in order to visualise a chaotic wave structure. Only one result is shown, as the effects of increasing the rotation rate on a chaotic flow are not especially obvious.

a.) **b.)** **c.)**

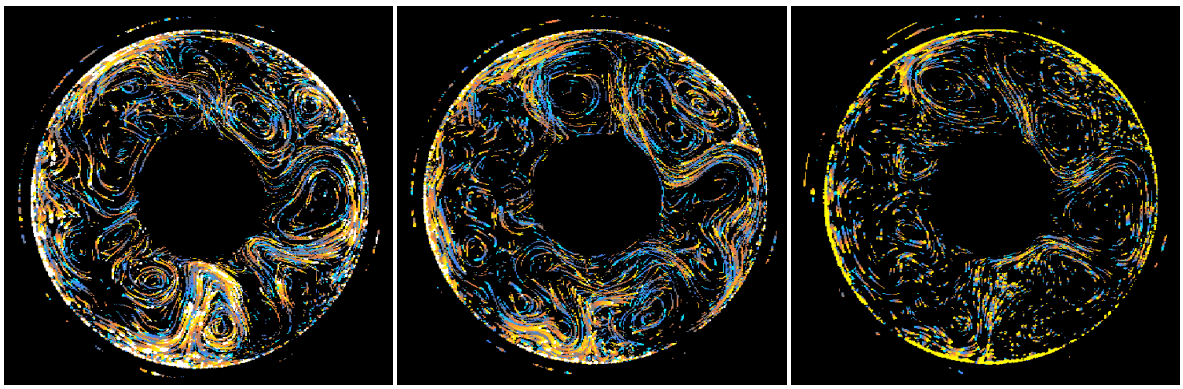

Figure 3.5: $\Omega = 2.75\ rads^{-1}$, $\Delta T = 5K$, $\mathcal{T} = 4.133x10^{8}$, $\theta = 5.655x10^{-2}$, *a.)* $t = 3600s$, *b.)* $t = 5400s$, *c.)* $t = 7200s$

With no consistency in space or time, Figure 3.5 is clearly part of the 'irregular' regime. Any recognisable wave structures, like the vague impression of a wavenumber-3 flow in the right hand side of Figure 3.5c, are brief in nature and are quickly returned to chaos. Bifurcations were not expected to occur within this region of parameter space and, indeed, no evidence of them can be observed.

3.1.3 Low Taylor Number

This run of experiments was devised to attempt to get as close to the bifurcation sequence as possible (see Figure 3.1), whilst still achieving adequate visualisation, by using the minimum temperature difference of 3 K found previously.

a.) **b.)** **c.)**

Figure 3.6: $\Omega = 0.6\ rads^{-1}$, $\Delta T = 3K$, $\mathcal{T} = 1.968x10^{7}$, $\theta = 0.713$, *a.)* $t = 3600s$, *b.)* $t = 5400s$, *c.)* $t = 7200s$

a.) **b.)** **c.)**

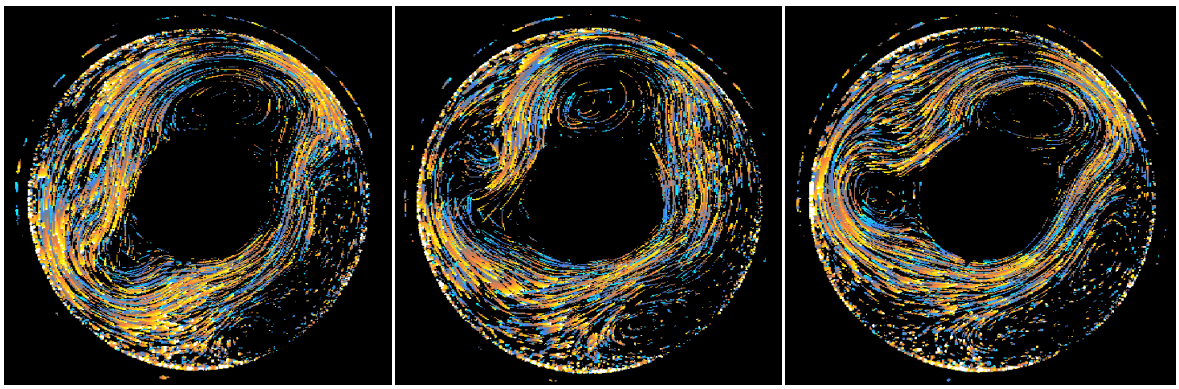

Figure 3.7: $\Omega = 0.7\ rads^{-1}$, $\Delta T = 3K$, $\mathcal{T} = 2.678x10^{7}$, $\theta = 0.524$, *a.)* $t = 3600s$, *b.)* $t = 5400s$, *c.)* $t = 7200s$

a.) **b.)** **c.)**

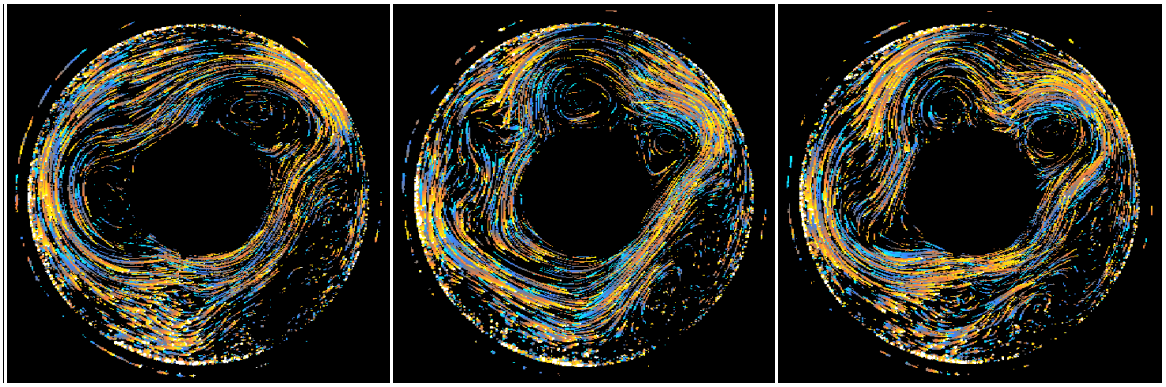

Figure 3.8: $\Omega = 0.8\ rads^{-1}$, $\Delta T = 3K$, $\mathcal{T} = 3.498x10^{7}$, $\theta = 0.401$, *a.)* $t = 3600s$, *b.)* $t = 5400s$, *c.)* $t = 7200s$

a.) **b.)** **c.)**

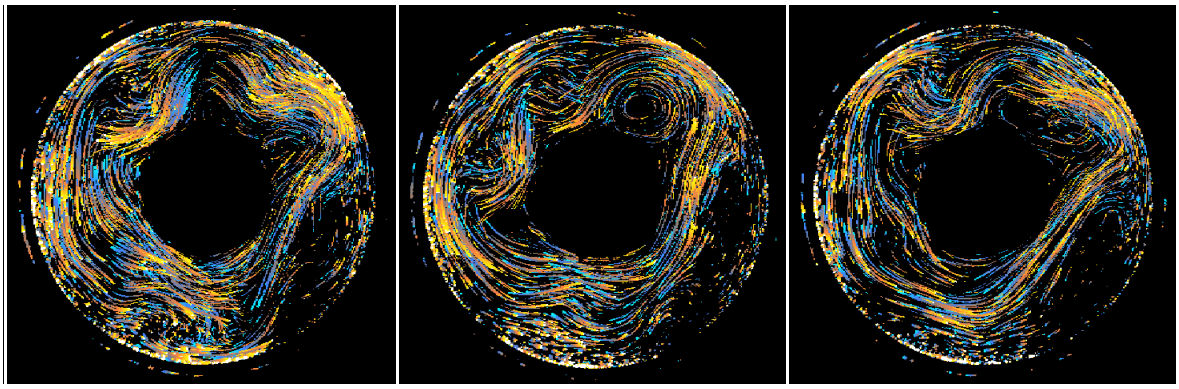

Figure 3.9: $\Omega = 0.9\ rads^{-1}$, $\Delta T = 3K$, $\mathcal{T} = 4.427x10^{7}$, $\theta = 0.317$, *a.)* $t = 3600s$, *b.)* $t = 5400s$, *c.)* $t = 7200s$

Figures 3.6 to 3.9 describe a region much closer to where Young and Read (2008) observed bifurcations in their experiments than the high Taylor Number flows. However, evidence of period-doubling is still noticeably absent. Furthermore, once again Figure 3.1 suggests that these locations in parameter space should be much steadier than what is observed, with only amplitude vacillation at most. Instead, every experiment appears to structurally vacillate between wavenumbers to some degree, and additional 'wave lobes' are surprisingly common. For example, Figure 3.8a shows a slightly skewed wavenumber-2, but 1800 s later in Figure 3.8b this has become a very atypical wavenumber-4. Another 1800 s in Figure 3.8c and the wavenumber-2 structure has returned, but with an obvious lobe at the top of the image. On the other hand, the results do show an increase in flow structure complexity as rotation rate is raised, with Figure 3.6 being closest to wavenumber-1, Figures 3.7 and 3.8 being closest to wavenumber-2 and Figure 3.9 being closest to wavenumber-3 structure.

3.1.4 Vector Velocity Diagram

As no evidence of bifurcations was found at any point in parameter space, it was decided to switch to the digital output signal anyway, and create an example vector velocity diagram of the flow. The point in parameter space (a rotation rate of 0.65 $rads^{-1}$ and 5 K temperature difference) was chosen as the flow structure was amongst the most simple found, and yet had enough particle saturation to produce a clear image.

A vector velocity diagram was created using CIV from two images with a time gap of one second between, immediately following the hour long spin-up time (3600 s). Clearly anomalous or 'false' vectors flagged by the software were manually removed, and Figure 3.10 was produced.

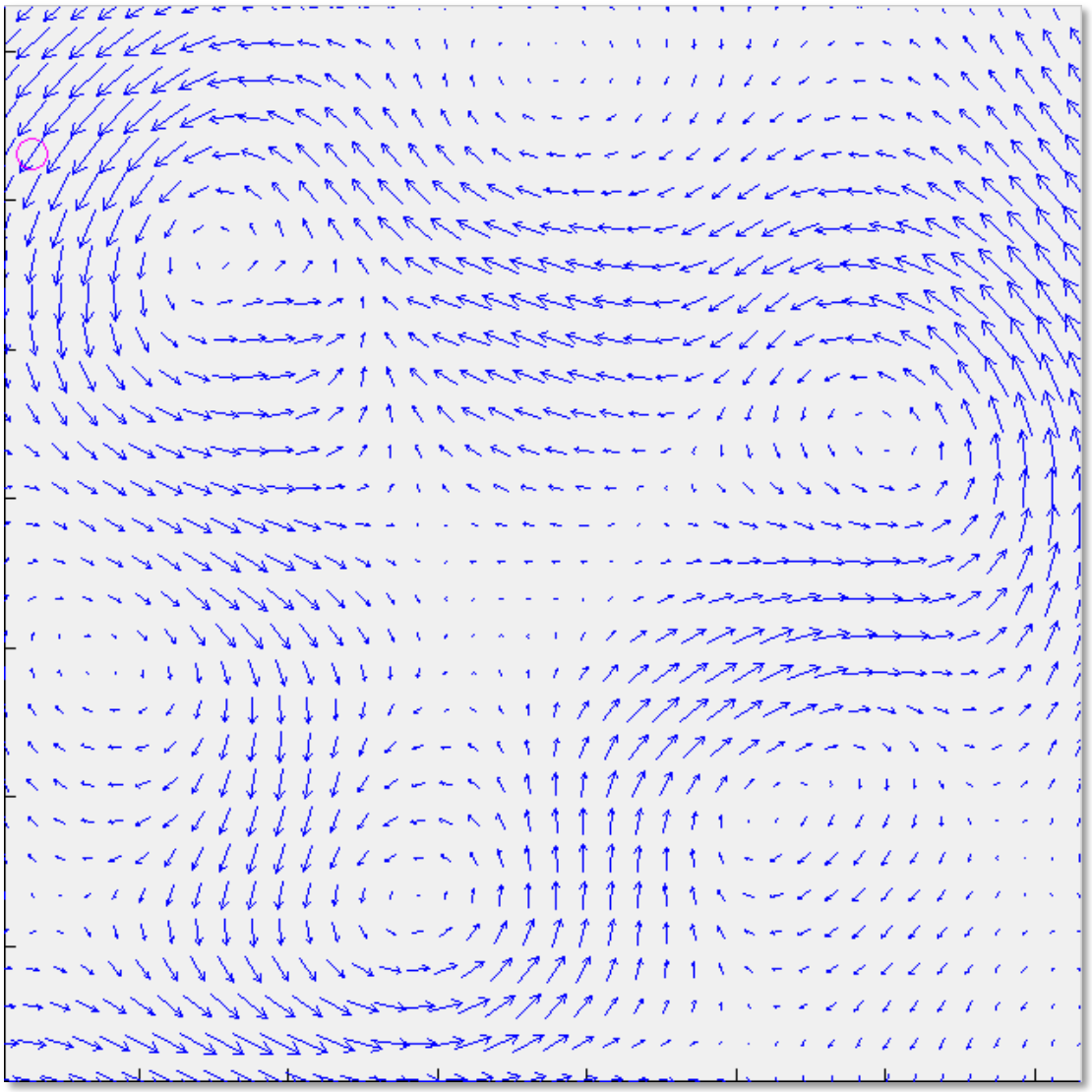

Figure 3.10: Horizontal vector velocity diagram. Parameters as in Figure 3.3a

To further illustrate the flow structure, a background of a sample image from the annulus was inverted and added to Figure 3.10, creating Figure 3.11. As CIV automatically 'completes' the flow field by inserting additional vectors where none were observed, a number of 'imaginary vectors' lying outside the bounds of the annulus were created. These have been removed from Figure 3.11.

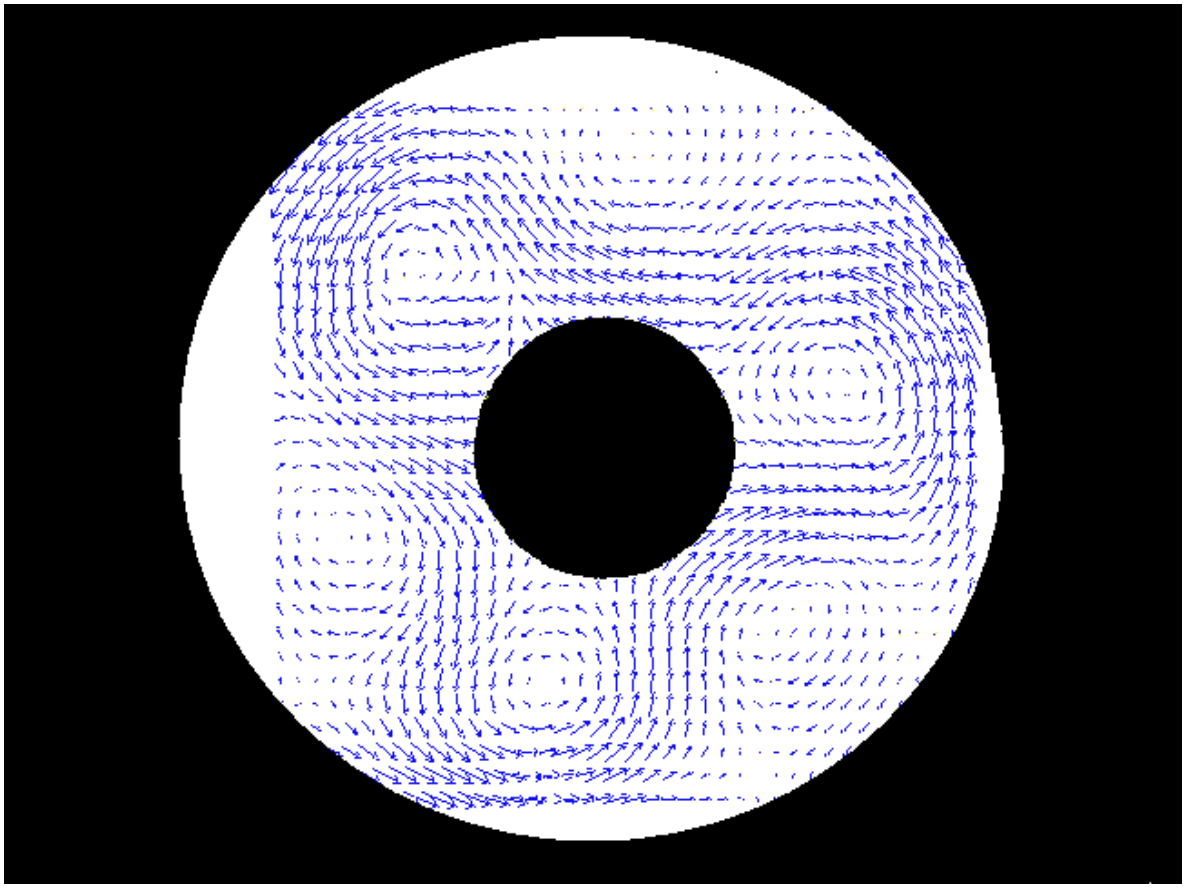

Figure 3.11: Vector velocity diagram with inverse background, showing where flow structure occurs in annulus. Parameters as in Figure 3.3a

Despite only being preliminary results, Figures 3.10 and 3.11 show extremely clear examples of a wavenumber-3 structure.

3.2 Analysis – Bifurcation Study

Although a large number of points in parameter space have been investigated, no evidence for bifurcations has been found so far. Referring to Figure 3.1, this is perhaps to be expected, as the bifurcation sequence found by Young and Read (2008) takes place over a very small area and is still an order of magnitude away in terms of Taylor Number from the nearest possible readings allowed for by the visualisation technique. More surprisingly, steady flow regimes have proved equally elusive, with some manner of structural vacillation occurring in all flows that were not fully irregular already (Figure 3.5). This vacillation can be seen even at low rotation rates and temperature differences, where previous studies[8] have consistently found steady wavenumbers, and is especially clear in Figure 3.3 where it can be observed that the flow first transitions between a wavenumber-2 and a wavenumber-3 (a), then between a wavenumber-1 and a wavenumber-2 (b), and then seems to be developing into a typical wavenumber-2 (c) over the course of the experiment. When the same conditions were repeated to create the vector velocity diagram, a typical wavenumber-3 regime was also found (Figures 3.10 and 3.11). It has been suggested that this is possibly due to the larger-than-standard annulus in use having an increased Rayleigh Number, a dimensionless number dependent on the on the scale of the gap between the inner and outer walls, defined for an annulus as:

$$Ra = \frac{\alpha \cdot g \cdot \Delta T (b-a)^3}{\nu \cdot \kappa} \tag{3.1}$$

This variation in Rayleigh Number could cause structural vacillation to occur at lower rotation rates and temperature differences than would be the case in a more standard size of annulus (Randriamampianina, private communication).

Alternatively, the additional wave-lobes and atypical structures may be due to another variety of period-doubling: *spatial period-doubling*. The difference between this and the temporal period-doubling of Young and Read (2008) is that the latter is primarily a route to chaos, whereas the former is caused by transitional instabilities. As explained in Rabaud and Couder (1983) and Chomaz et al (1988), who used films of soap trapped between two plates as their working fluids, spatial period-doubling is generated by non-linear interactions between the main wave structure and its lesser harmonics. For example, Figure 3.3b could be described as the superposition of a dominant wavenumber-2 and a harmonic wavenumber-1 flow. This fits well with the findings of the soap experiments, despite those period-doubling regimes being at much greater wavenumbers, due to the differences in apparatus and approach.

[8] Hignett et al (1985), for instance.

3.3 Inertia-Gravity Wave Study

In this section, figures are provided for whenever instability rolls were observed (or, more accurately, whenever they could be picked up by the camera). When rolls were not observed directly, a short explanation is given, describing what the tracer dye did instead. For the Figures where the rolls were found, estimations of the roll size and the depth from the surface that the instability begins at are given, as well as the rotation rate, temperature difference, Taylor Number and Rossby Number (dimensionless numbers calculated to 3d.p.). Marking the inner cylinder with height indicators proved to be problematic, so a simple calibration image was taken by holding a ruler up against the wall. This calibration image is provided in Figure 3.12.

Figure 3.12: Simple calibration image for determining depth and size of waves (ruler starts at base of annulus, reading 50cm)

3.3.1 Water Experiments

For the first result only, three images will be given instead of one. This will allow for visualisation of the formation and evolution of the instability roll. The other results (where the instability is harder to observe) will show the final structure of the roll, equivalent to the third image, permitting the magnitude of the wave within the thermal boundary layer to be measured. To indicate the area where the roll is taking place, a blue box has been added to each image.

a.) **b.)** **c.)**

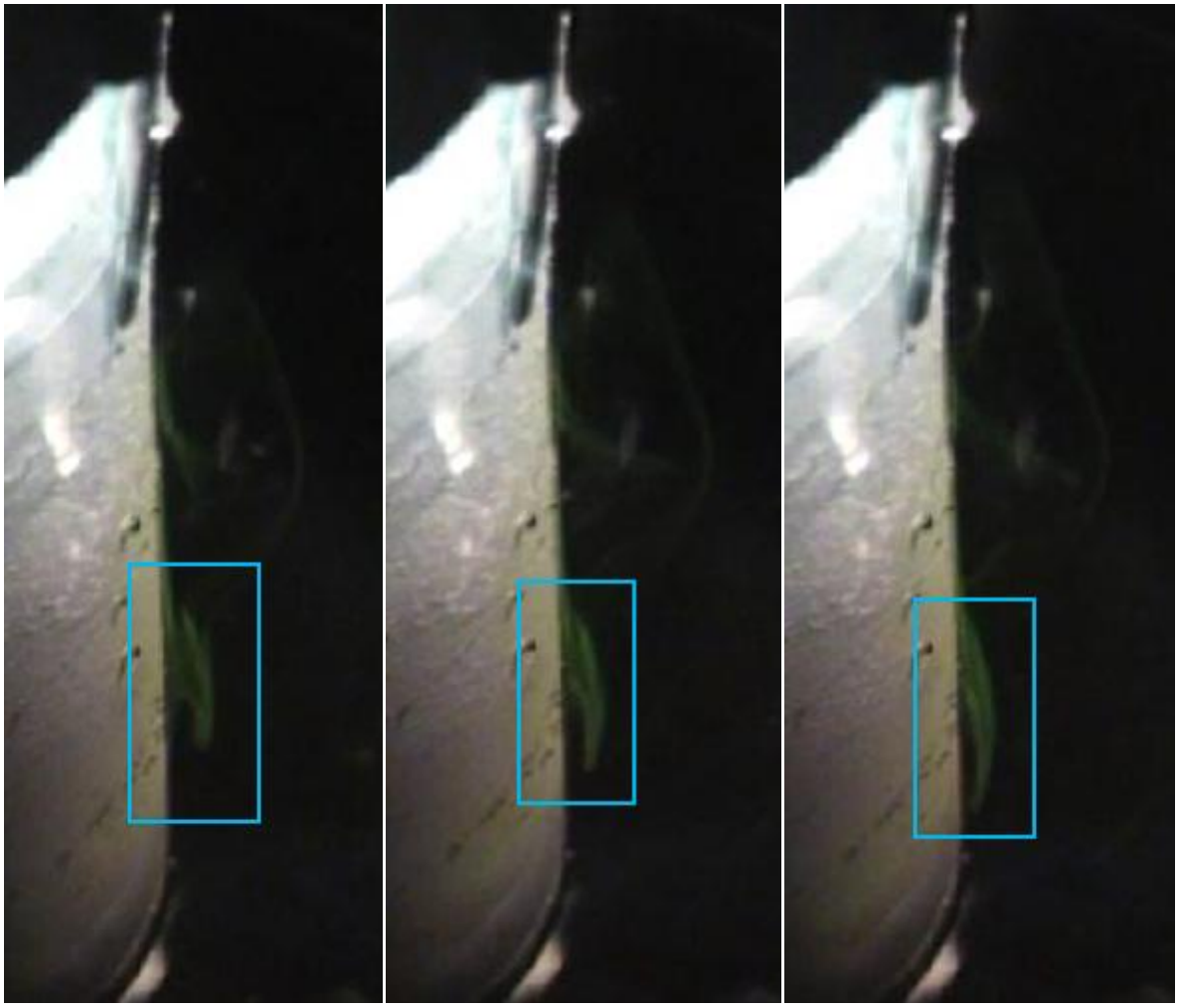

Figure 3.13: $\Omega = 1$ *rads*$^{-1}$, $\Delta T = 2$ *K*, $\mathcal{T} = 1.380x10^{8}$, $\theta = 0.112$, *roll size (from c) = 10 cm, depth = 12 cm*

The Figure 3.13a shows the tracer leaving the inner wall and beginning to form a roll. In Figure 3.13b, the instability continues descending through the annulus, before the roll curves back and re-joins the inner wall in Figure 3.13c.

a.) **b.)** **c.)**

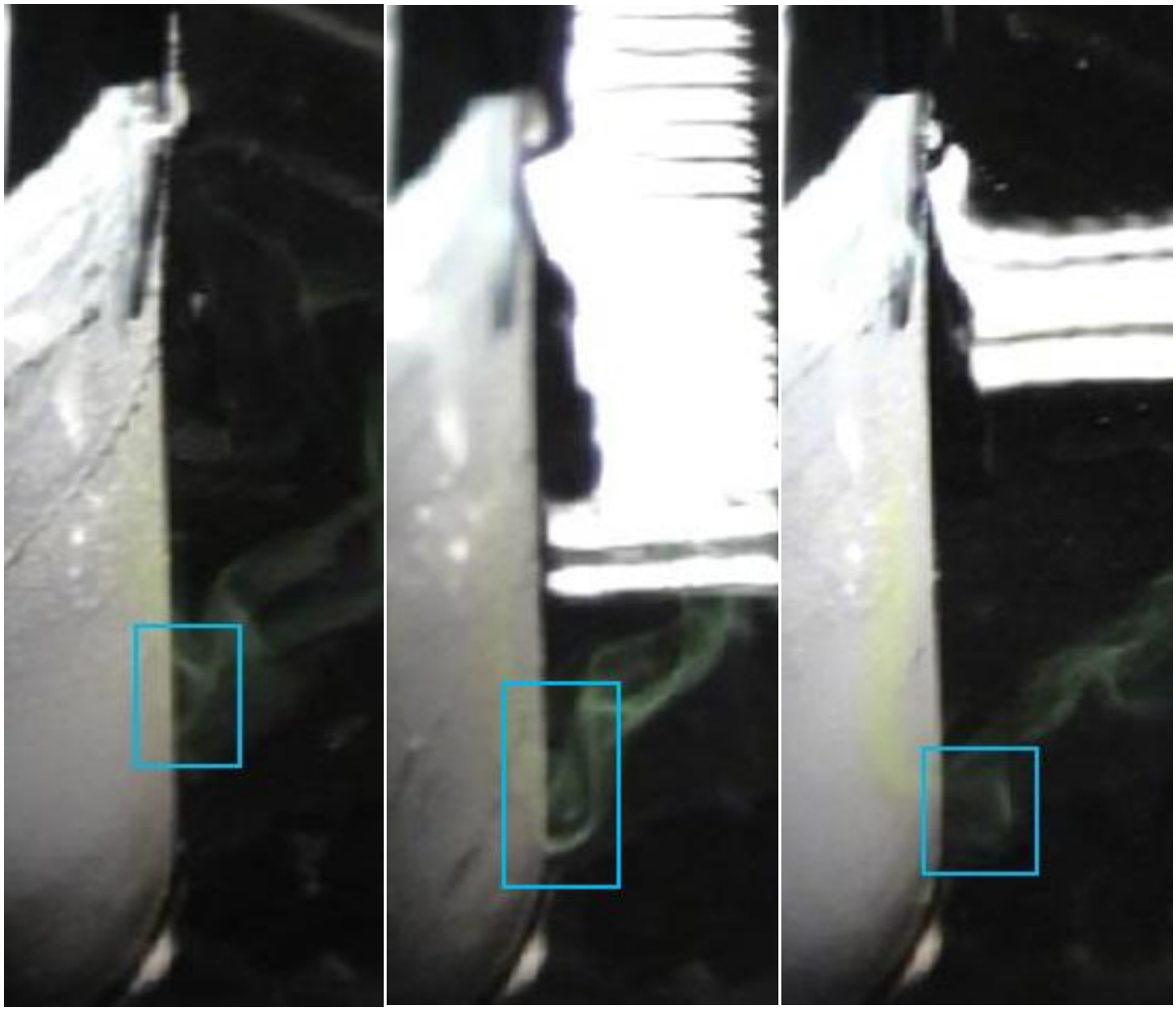

Figure 3.14: a.) $\Omega = 0.8$ *rads*$^{-1}$, $\Delta T = 2$ *K*, $\mathcal{T} = 8.829x10^{8}$, $\theta = 0.175$, *roll size = 4 cm, depth = 15 cm, b.)* $\Omega = 1$ *rads*$^{-1}$, $\Delta T = 5$ *K*, $\mathcal{T} = 1.380x10^{8}$, $\theta = 0.280$, *roll size = 12 cm, depth = 13 cm, c.)* $\Omega = 0.8$ *rads*$^{-1}$, $\Delta T = 5$ *K*, $\mathcal{T} = 8.829x10^{8}$, $\theta = 0.438$, *roll size = 5 cm, depth = 20 cm*

In Figure 3.14, the tracer can be observed to follow the expected behaviour for a stationary inertia-gravity wave, as described in Chapter 1. The dye within the thermal boundary layer descends vertically before encountering an instability roll in the lower half of the annulus. After extending a small amount towards the outer wall, the roll causes the tracer to return to the inner cylinder until the flow reaches the base. Multiple rolls, on the other hand, were not observed under any conditions, even in cases where the dye remained visible within the boundary layer all the way to the bottom.

At a rotation rate of 0.6 $rads^{-1}$ and 2 K temperature difference no instability roll was observed by camera or by eye. It was assumed that this implied that the rotational forcing at this rotation speed was too small to allow inertia-gravity waves to form within the thermal boundary layer. In addition, when the temperature difference was increased to 5 K, the result remained the same. This in turn suggested that 0.6 $rads^{-1}$ is too low a rotation rate for visible inertia-gravity waves, regardless of the amount of thermal forcing.

In all experiments at the 10 K temperature difference, no viable readings were made. Due to the large thermal forcing, the baroclinic waves were much more intense than in previous experiments, and acted to drag the tracer away from the inner wall. The amount of dye that was able to remain within the thermal boundary layer was too little to observe any instabilities. It is unknown, therefore, whether inertia-gravity waves can occur under these conditions. The results of Jacoby et al (2010) suggest that they should exist, but without further experiments this hypothesis would be impossible to verify.

3.3.2 Water-Glycerol Mixture Experiments

Unfortunately, at this time, all experiments with a water-glycerol mixture as the working fluid were unsuccessful. This was due to a new and foreseen problem: the relative density of the tracer dye. Despite the Fluorescein sodium having been made up in a solution of water-glycerol with the same density as the working fluid, when the dye was injected into the annulus it immediately floated to the surface. It was suggested that this could be due to a small discrepancy in the density of the fluid nearest the inner wall, where the cooling surface may fractionally increase the density of the surrounding liquid. To compensate for this, the dye was re-created with slightly more glycerol in the mixture, but this caused the opposite problem: the tracer descended rapidly down the boundary layer and reached the base of the annulus before any instability roll could be set up. Due to time restraints, any further experiments into inertia-gravity waves with water-glycerol mixture will have to form future work in subsequent years of this thesis.

3.4 Analysis - Inertia-Gravity Wave Study

In the water experiments, stationary rolls were observed, as expected. However, with the lack of the water-glycerol mixture experiments, no drifting rolls could be witnessed. By comparing Figures 3.13 and 3.14b (1 $rads^{-1}$) to Figures 3.14a and 3.14c (0.8 $rads^{-1}$), it can be observed that, as the rotation rate decreases, the instability rolls get smaller and more difficult to see. Similarly, by comparing Figures 3.13 and 3.14a (2 K) to Figures 3.14b and 3.14c (5 K), it can be observed that, as the temperature difference increases, the rolls occur closer to the base of the annulus. Even through the roll in Figure 3.14b begins at a slightly higher depth than the roll in Figure 3.14a, the former is much larger, and terminates very close to the base of the annulus. The absence of multiple rolls is surprising, but is possibly due to the secondary rolls either being too small to be seen, or occurring too low in the annulus to be discernable from the dye encountering the base.

Chapter 4

Preliminary Conclusions

In this chapter the various results and observations of Chapter 3 will be examined in greater detail, with a discussion on what has been learnt from both studies. A section will then highlight the outstanding issues of the first-year experiments, both in terms of possible methods to observe phenomena that were not encountered with the current arrangement and further extensions to the studies to investigate other aspects of bifurcations and inertia-gravity waves.

4.1 Discussion – Bifurcation Study

The major conclusion of the bifurcation study is that, due to the large annulus in use, structural vacillation is a regular occurrence at most points in the observed parameter space. This indicates that the current position of investigation is too far from the bifurcation sequence (Figure 3.1). In addition, Young and Read's (2008) bifurcations were found to occur within the wavenumber-2 amplitude vacillation region. Despite some results (Figure 3.4, for example) showing reasonably steady drifting wavenumber-2 structures, the prevalence of structural vacillation in the rest of the experiments meant that the location of this region remained elusive, let alone the tiny area within this region containing the supposed bifurcation sequence. A further problem is that, if temperature difference and rotation rate are reduced to get closer to the bifurcations, the weak baroclinic waves evoked would not be enough to allow particles to saturate the flow and be visible. With the current arrangement of annulus and visualisation technique, temporal period-doubling appears to be impractical to investigate.

On the other hand, the results gathered bear some resemblance to spatial period-doubling was discovered. This is an interesting phenomenon in its own right, despite having been observed in laboratory research before, and further study could be achieved by carrying out more experiments in the same parameter space, finding the limits of where spatial period-doubling occurs.

As a tertiary finding, above a temperature difference of 3 K it was established that the particle tracking software could produce good quality images of vector velocities (Figures 3.10 and 3.11). The visualisation equipment and software used are therefore clearly viable for results gathering in the subsequent years of this thesis.

4.2 Discussion – Inertia-Gravity Wave Study

The inertia-gravity wave study was the notably more successful of the two investigations. Instability rolls were observed in a laboratory setting, and a reasonable visualisation of the thermal boundary layer structure was achieved (Figure 3.13). It was also found that decreasing the rotation rate reduces the size of the instability rolls, whilst increasing the temperature difference causes the rolls to occur at a greater depth, verifying the numerical results of Jacoby et al (2010). These findings are only qualitative, however, as the measurement system employed was limited in accuracy (Figure 3.12). In addition, it was discovered that there is a minimum rotation rate required for instability rolls to exist, as none were encountered at 0.6 $rads^{-1}$. Instability rolls were also not encountered at the highest temperature difference of 10 K, but it is currently unknown whether this is the 'true' result or due to experimental problems.

The foremost weakness of the study was that the water-glycerol mixture experiments had to be abandoned due to time constraints. As such, no drifting instability rolls could be observed and no comparison could be made between the fluids. Furthermore, only single rolls were found in the water experiments, not the expected multiple rolls.

4.3 Outstanding Issues

The solution to the problems of the bifurcation study is to carry out the investigation again, this time employing a smaller annulus, more like that of Young and Read (2008). Hence, the change in Rayleigh Number would be nullified, and the rotation rates and temperature differences would be easier to match up to the numerical work (they would not be same due to the change in the value for viscosity). The same methodology could be utilized as in Chapter 2, with Digimage used to find the bifurcations and CIV used to create delay coordinate reconstructions. If the results of Young and Read (2008) are verified, further experiments can be devised.

Alternatively, instead of a different annulus, a different visualisation technique could be employed. Rather than using tracer particles and a camera to create velocity data, an array of thermocouples could produce temperature data. For a useful profile, however, they would be required to extend into the flow, much like the arrangement of Leach (1981). This would have an impact on the flow, but could be reduced with careful construction. Additionally, temperature data should be actually much better for modal analysis, not least because of the ability to take readings over the entire depth of the annulus simultaneously. Apart from the difference in data, the methodology would be unchanged.

For the inertia-gravity wave study, the equipment arrangement could be improved with a better lighting system and by using a longer needle to inject the dye deeper in the thermal boundary layer (where, hopefully, more of it would remain, leading to better visualisation). This could permit readings at high thermal forcing, assuming the problem is purely the lack of tracer in the layer, and even investigation of multiple instability rolls, if the issue is successive rolls being too small to see. If multiple rolls are still not observed after these alterations, weaker thermal and rotational forcing may be needed, causing larger rolls that occur higher in the annulus. A more accurate measurement technique would also allow for quantitative results.

In order to carry out the water-glycerol mixture investigation, it would be necessary to first perform many experiments to determine the exact ratio between water and glycerol needed to create dye that is neutrally buoyant in the thermal boundary layer. Once this is achieved, drifting inertia-gravity waves can be studied, with further improvements to the apparatus, if needed.

The exact critical value for minimum rotation rate could be discovered with further experiments between 0.6 and 0.8 $rads^{-1}$ (for water), especially with the ability to vary the rotation rate continuously. Similarly, the same technique could be used to investigate the minimum temperature difference required, as well as the maximum values of both parameters, should they exist.

Lastly, experiments could be repeated with a lid featuring a hole for the needle, allowing the effects of wind stresses to be investigated.

Chapter 5

Topographic Review

As described in Chapter 1, another major aspect of sloping convection and atmospheric circulation in general is that of topography. As such, the second and third years of this thesis will be spent investigating the effects of topography on the atmospheric circulation using the differentially heated annulus described in Chapter 2. This chapter will therefore give a brief review of the topic, beginning with an assessment of the various unresolved questions found within the literature. Of these problems, the most interesting (and most applicable to the annulus) will be looked at in greater detail, forming an initial outline of the experiments to be carried out in the subsequent years of this study. This will be followed by a description of how the apparatus of this thesis will be altered to allow for topographic study, as well as improvements to increase the accuracy and clarity of the results.

5.1 Topographic Problems

Within the literature on the topic of topography there are several open questions that have yet to be resolved. In this section, several of the most pressing of these will be studied, looking at the original papers that raised them, any further development in subsequent works, and how the questions could possibly be answered in a thermally-driven annulus.

Possibly the most major question found in the literature is the issue of the existence of multiple equilibria. Most notably, Charney and DeVore (1979), Charney and Straus (1980) and Reinhold and Pierrehumbert (1982) suggested the idea that both the ‘low-index’ (blocking) and ‘high-index’ (zonal) regimes (caused by non-linear interactions between the background zonal flow and bottom topography) are meta-stable and can both exist under the same conditions. Transitions between the regimes are caused by barotropic instabilities of the topographic wave and, in turn, cause most of the atmospheric anomalies that are observed.

On the other hand, Tung and Rosenthal (1985) and Cehelsky and Tung (1987) claimed that multiple equilibria are physically possible, but cannot exist in the real atmosphere. They suggested that previous results of multiple equilibria were caused by unrealistic topography or, in the case of Charney, Shukla and Mo (1981) where the topography used is deemed to be sufficiently ‘realistic’

(illustrated in Figure 5.1), overly-truncated non-linear interactions. In their models, asserted to be better analogies to the atmosphere, no multiple equilibria are found and the regimes are solitary. The flaw of these papers is that no definition of what is meant by 'realistic' topography is given. Sometimes it appears they are suggesting that topography in previous studies was overly large, but that of Charney, Shukla and Mo (1981) is similar in scale to that of Charney and DeVore (1979). As such, it will be assumed that by 'realistic', they mean a complex topography closer to the distribution of mountains on Earth.

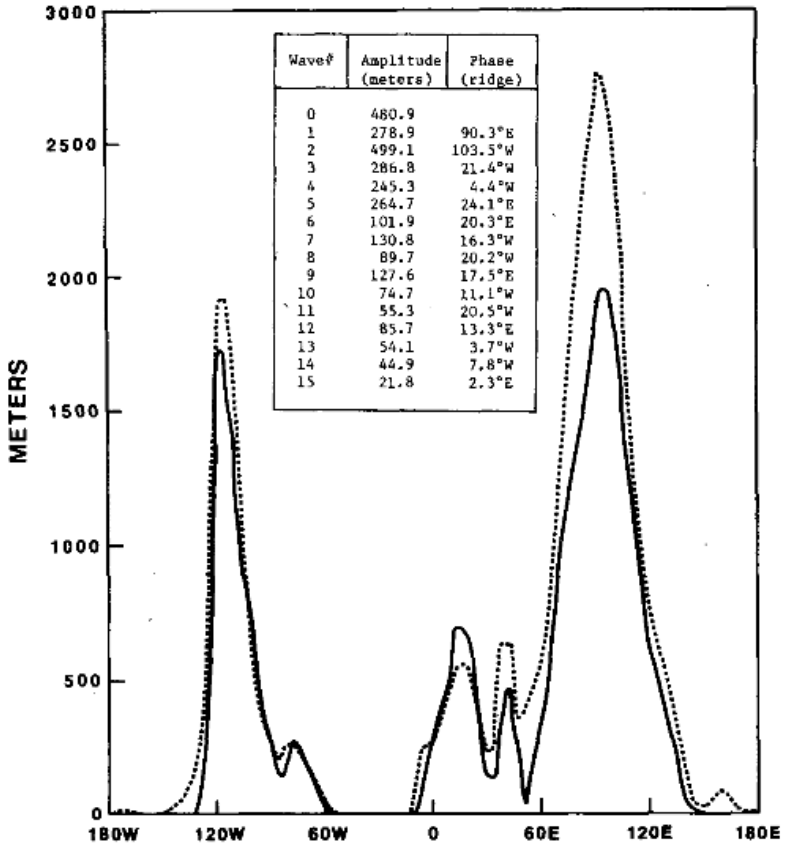

Figure 5.1: 'Realistic' topography, dotted line created from actual topographic measurements [from Charney, Shukla and Mo (1981)]

These papers were in turn rebuffed by Molteni (1996) using high-resolution hemispheric models. Contrary to Tung and Rosenthal (1985) and Cehelsky and Tung (1987), two distinct flow regimes were found, even when a large enough number of degrees of freedom were used to simulate fully non-linear interactions. However, since simple wavenumber-3 topography is employed, it could be argued that multiple equilibria has only been shown to be possible with this type of topography, and furthermore that this model is not 'realistic' enough to be applied to the real atmosphere.

Similarly, Risch (1999) claimed to find laboratory evidence for multiple equilibria in a thermally-forced annulus for both with and without topography. The topography used was a simple wavenumber-2 shape, suggesting that (like in Molteni (1996), above) low-order models that found multiple equilibria with similar topography were not seeing a false positive due to their 'overly-truncated non-linear interactions', as alleged by Tung and Rosenthal (1985) and Cehelsky and Tung (1987). By extension, Risch (1999) notes that this implies that multiple equilibria should also be possible in the baroclinic atmosphere. The need for 'realistic' topography is still an issue, however.

Supporting the other side of the argument, Tian et al (2001)[9] compared similar numerical and laboratory annulus studies, finding stable multiple equilibria to be prevalent in the former, but not to exist at all in the latter. The physical annulus still produced both zonal and blocked regimes, but they were meta-stable, with irregular, sudden transitions. The lack of multiple equilibria could be due to the fact that the annulus is barotropic (forced by jets) as well as the topography being a simple wavenumber-2 type. No transitions were observed in the computational model, possibly due to the lack of three-dimensional effects (this is to be verified via further numerical simulations).

Recent works, such as Koo and Ghil (2002) and others by the same authors, claim that multiple equilibria can be observed in their models with realistic topography and fully-realised non-linearity. However, the study is, by the authors' own admission, carried out on a low-order model.

In an annulus, though the atmospheric model is simplistic, the non-linear interactions will not be truncated, giving a perfectly 'realistic' flow. Unfortunately, creating 'realistic' topography is more difficult than in a numerical model, especially if fine features are required. If this problem can be overcome, the topography of Charney, Shukla and Mo (1981) can be recreated – with this 'realistic' topography and the fully non-linear interactions of a physical annulus, a definitive investigation into the existence of multiple equilibria could be launched, putting to the test every condition of Tung and Rosenthal (1985) and Cehelsky and Tung (1987) simultaneously.

By going one step further, this could become a new experiment in its own right: carrying out a simple study with basic wavenumber-2 type topography, and then replacing the bottom surface with increasingly more complex mountain distributions (different elevations, asymmetrical locations, lesser peaks etc) until no further difference between results can be detected. This would give a reasonable definition for a 'realistic' topography and could then be applied to the investigation into multiple equilibria as a future study. Naturally, this experiment would be easier for a computational model, to save having to build many different iterations of the topography, as well as removing the time-consuming task of emptying and refilling the annulus every time each new topography was used.

[9] This paper appears to change the meaning of 'meta-stable' from '*can* transition from one regime to another', to '*will* transition between the regimes'. Hence, the 'meta-stable' states in Charney and DeVore (1979), that allow multiple equilibria, are re-classified as 'stable' by Tian et al (2001).

However, the benefits of finding a compromise between realism and manufacturing difficulty could lead to the creation of a standard 'Earth' topography for use in many future annuli studies.

In a similar vein to the search for 'realistic' topography, an unresolved question exists in what type of topography should be employed. Practically all differentially heated annuli use sinusoidal topography. However, this can range from a simple wavenumber-2 type, as seen in Bernardet et al (1990), through a simple wavenumber-3 type shown in Risch (1999), to a non-axisymmetric wavenumber-5 type, found in Jonas (1981). A further option is for radial variation: Li, Kung and Pfeffer (1986) carried out experiments with radially uniform topography, but Leach (1981) included a slope so that his topography was greater near to the outer wall.

In numerical studies as well, a sinusoidal bottom surface as shown in Charney and DeVore (1979) is the most common. Again there is no standard, and both wavenumber-2, as in Li, Kung and Pfeffer (1986), and wavenumber-3, as in Molteni (1996), types are widespread, due to similarities to the topographies of Earth and Mars. Less regular shapes are also possible, such as Yang, Reinhold and Källén's (1997) single isolated mountain and Charney, Shukla and Mo's (1981) uneven topographic distribution based on actual measurements of Earth's mountain ranges.

Which choices are made are up to each individual author's judgement of what arrangement of equipment creates a good simulation of the atmospheric circulation without over-simplification or over-complication. However, it stands to reason that some types of topography will produce better simulations of the Earth (or whichever planet is the focus of interest) than others. This leads back to the concept of the search for a standard 'Earth' topography – experiments could determine whether radially uniform or radially sloped topography (for example) was a better compromise between realism and manufacturing difficulty, and thus declare that to be the superior representation.

A number of unresolved questions about the effects of topography on the atmosphere could be posed on the more unusual findings of Risch (1999). A strange occurrence was found whereby, for low Taylor number and medium Rossby number flows, a wave-3 stationary wave was found to grow a fourth 'wave-lobe' (Figure 5.2) at low levels, but not at high levels. This could possibly be showing an example of blocking, and could be examined via further study of that region of parameter space. A second question concerns the understanding of stratospheric sudden warmings, a mysterious phenomena of the atmosphere, although they are known to be caused by seasonal variations. Changing the temperature difference over longer time-scales could mimic these seasonal variations, thus leading to a study of stratospheric sudden warmings. Finally, a lesser question is the relative

scales of the effects of thermal and topographic forcing on the rise of stationary waves. This could be investigated by using insulating material (or similar) to only allow a temperature difference on the upper half of the annulus, hence comparing the thermally-forced upper half to the topographically-forced lower half.

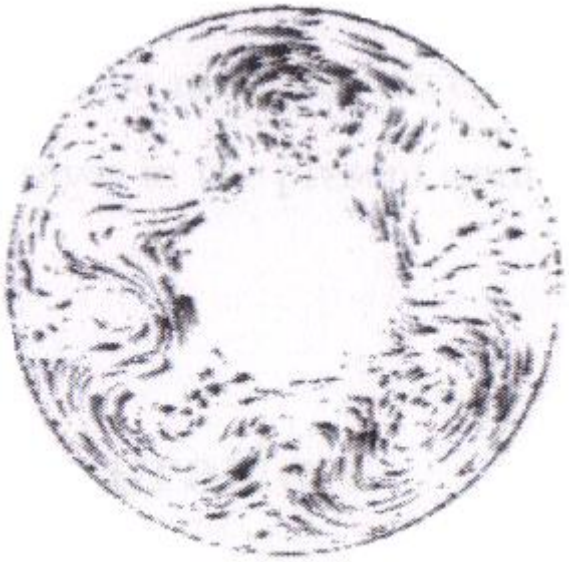

Figure 5.2: Wavenumber-3 structure with rogue 'wave-lobe' at low level, $\mathcal{T} = 1.2x10^6$ [from Risch (1999)]

Unfortunately, without a re-design of the annulus, the addition of insulating material for the forcing comparison experiment would cause interference with the flow, unless the material was very thin, at which point the insulating properties may not be strong enough to separate the thermal forcing. A fair amount of work would be needed to rectify this. The investigation into seasonal variations seems more feasible, with it also appearing to be a more interesting area of research and the most relevant to the atmosphere. Additionally, improving a laboratory study so that it more closely resembles the long-term atmospheric circulation would allow for study of oscillations with much longer periods than currently possible in a physical annulus. The rogue 'wave-lobe' discovered bears some similarity to the findings of the bifurcation study, so spatial period-doubling may be a cause. Future experiments with the same apparatus should be able to investigate this possibility further, particularly when images can be taken from all levels.

A more mathematical unresolved question, based on the comments of Benzi et al (1986), is that there is difficulty in writing a single equation for the zonal flow over topography. This is due to a poor assumption for the calculation of form drag, a complicated feedback between topography waves and zonal wind, and the fact that non-geostrophic effects (such as boundary layer separation and topography steepness) are ignored.

Whilst form drag is a very interesting aspect of topography, with numerous parallels to other topics in fluid dynamics including nautical and aerospace engineering, a laboratory study such as an annulus cannot give an equation for zonal wind directly, like a numerical model could. However, a physical study could shed some light on which non-geostrophic parameters affect zonal wind, and by how much. In addition, if time permits, the planned numerical study for the subsequent years of this thesis (see Chapter 6) may be adapted to attempt to answer this question.

A recent open question concerns the origin of Low-Frequency Variability (alternatively Low-Frequency Vacillation, shortened to LFV). LFV is defined by Koo and Ghil (2002) as the variability of the atmosphere with a time scale longer than major weather phenomena (5-6 days) but shorter than seasonal variability (about 100 days). Naturally, this means that the variability is extremely important for weather predictions and forecasting. The authors state that it is dominated by atmospheric zonal flow vacillation, and that it is often caused by non-linear interactions and transitions between multiple equilibria regimes, but the precise mechanism for its formation is still unresolved.

In a related subject to the above, Ghil and Robertson (2002) divided the topic of LFV into planetary flow regimes ("particles") and intraseasonal oscillations ("waves"). They state that it is unknown whether the former are slow phases of the latter, or the latter are instabilities of the former. The authors note that both are fundamentally important, and knowing their relationship will greatly increase predictability of the atmosphere.

Kondrashov, Ide and Ghil (2004) revisited this latter issue, seemingly leaning towards the idea that the slow phases of the oscillations denote the locations of the unstable equilibria, but decide that an in-depth analysis is "beyond the purpose of the present paper".

The origins and internal relationships of LFV would be a difficult question to answer in an annulus, though the topographically forced oscillatory instability discussed by Ghil and associates could be looked at in further detail. The transitions between regimes in the annulus and their counterparts in the atmosphere could also be studied, perhaps as part of a larger study into multiple equilibria.

Despite plentiful research in the area, a question remains of the precise effects of adding a small amount of topographic variation, as opposed to a flow over a flat surface. One of the most surprising and unusual effects of topography known from numerical models, for example Charney and DeVore (1979), is that low topography can actually act to stabilise a given flow, requiring a greater thermal forcing (or rotation rate, depending on what parameter is held constant) to produce instabilities. Cehelsky and Tung (1987) provide Figure 5.3 to illustrate this concept.

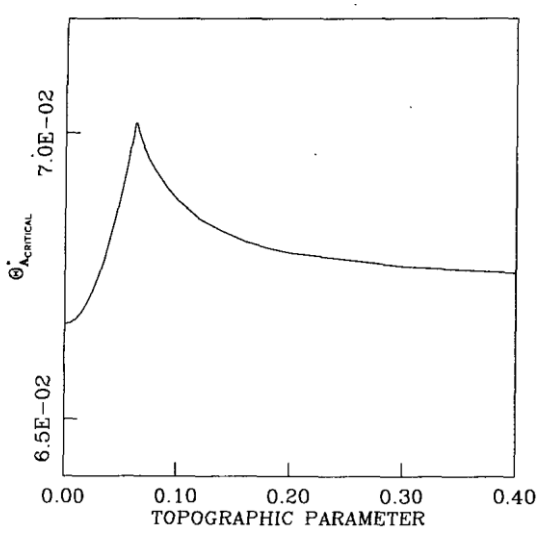

Figure 5.3: Representation of flow stability (represented by the y-axis, a higher value implying greater stability) against topographic height showing initial stabilisation and peak at low topography [from Cehelsky and Tung (1987)]

Jonas (1981) was the first to attempt to apply this effect to a physical annulus, using an increase in rotation rate rather than an increase in thermal forcing. Using a simple analysis, the author predicted the effects of the addition of topography, including an increase in rotation needed before the transition to baroclinic waves is reached, an increase in wavenumber of these waves and a decrease in length of the baroclinic waves. The predictions were backed up by the observations taken, but only qualitatively. The author noted that the analysis is "grossly inaccurate" when applied to the real annulus, not least because boundary-layer separation (which would imply zero vertical velocity at the top and bottom) cannot be observed. He also mentioned that: "calculations of the spatial growth rates of perturbations in flows of spatially varying static stability would provide useful information on this mechanism".

Both blocking and zonal flow regimes were investigated in Tian et al (2000), with focus on their spatial and temporal characteristics. A numerical study is compared with a laboratory annulus, noting the spatial similarity of both experiments, including the shape and location of the flow vortices and the configuration and magnitude of the jet. No growth rate is given, however, and the annulus is

barotropic – forced by rings of holes between the topography that pump in fluid to create an eastward jet.

As such, there is plenty of scope to investigate Jonas' (1981) findings with a differentially heated baroclinic annulus, focussing on the study of the spatial growth rates of the perturbations evoked. As noted by Jonas, it is very difficult to explore the separation at the boundary layers, but could be achieved (in a re-designed annulus) by having a lighting layer very close to the top or bottom of the fluid, and perhaps utilising an angled camera, such as in the boundary layer study. This solution would have further problems, such as reflections from the lid, but would make for an interesting, if complicated, investigation.

As mentioned, Tian et al (2001) carried out their research with a different type of annulus – the barotropic annulus, shown in Figure 5.4. Instead of setting up convection via a temperature difference, a barotropic annulus creates a flow by pumping fluid through several concentric rings of holes that lie between the topographic peaks and troughs. This has the effect of removing any vertical variation and is employed when the stratification of the atmosphere is deemed negligible. Naturally, this removes complexity from the model, allowing other phenomena to be more easily observed.

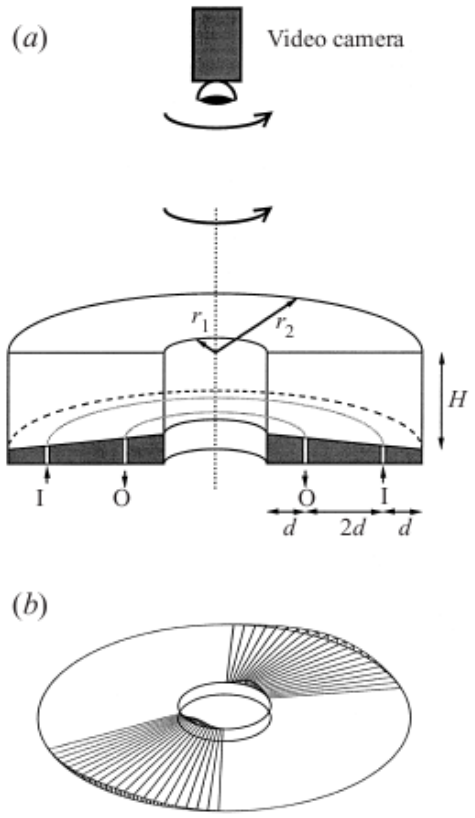

Figure 5.4: Barotropic annulus with sloping base a.) shows typical laboratory arrangement, b.) shows concentric rings of hole for pumping of fluid [from Tian et al (2001)]

The numerical equivalent to the barotropic annulus is the one-layer model, compared to the two-layer baroclinic model. One-layer models reduce the simulation to barotropic to decrease computational expense when vertical structure is not needed. This type of model is almost as common as the two-layer type, with examples occurring in Charney and DeVore (1979) and Benzi et al (1986). One-layer models also appear to be the standard for studies of Martian topography, with both Keppenne (1992) and Keppenne and Ingersoll (1995) using barotropic shallow-water experiments in their papers.

This raises the obvious question – how far do barotropic and baroclinic models with topography differ? Furthermore, how does adding baroclinic structure affect the results of barotropic models? This could be investigated by replicating the results of Tian et al (2001) in a baroclinic annulus, or by using a one-layer numerical model under the same parameters as an annulus experiment.

Finally, it should be noted that, since the focus of this project is the interactions of topography with the atmospheric circulation, the majority of the literature examined is based on the dynamics of the atmosphere. The oceans experience topography as well and there is plenty of scope for comparison between the two. One of the major differences is the forcing of the flow: atmospheric studies, like all those mentioned above, are thermally-driven; oceanic studies, like Völker (1999) who simulated the Antarctic Circumpolar Circulation, are wind-driven. Without that distinction, the latter's study is difficult to distinguish from a standard atmospheric study, employing a baroclinic quasi-geostrophic channel model.

This being the case, it would form an interesting study to compare the oceans and the atmosphere within the annulus. This could be achieved by creating simple ocean-like topography, for example tall 'blocks' that could be dropped into the annulus, trapping the bottom layer, like the ocean basin experiments of Wordsworth (2008), except in that case the vertical walls used blocked the entire depth of the fluid. Alternatively, the ocean forcing could be simulated by replacing the heating and cooling systems with an array of fans to drive the flow. The current annulus in use would probably not make the best choice for either of these options (especially not the latter) due to its large size, but a smaller annulus could be converted relatively quickly and easily.

5.2 Proposed Topographic Study

In conclusion, the existence of multiple equilibria is still the biggest unresolved question in topography, even if it is not as controversial a topic as it once was in the period after Tung and Rosenthal (1985) and Cehelsky and Tung (1987) published their papers. However, the most immediate aspect of this issue is how best to create a topography for an annulus that can be defined as 'realistic'. For the sake of clarity, instead of the term 'realistic', from now on the topography investigated will be referred to as 'less-idealised'. This issue was brought up in Li, Kung and Pfeffer (1986). In that paper, a simple wavenumber-2 type topography was employed, but it is noted that the real topographic distribution of Earth (and other planets) is much more complicated. The authors expressed a wish to repeat their experiments with a better model of this distribution, suggesting a superposition of the Fourier components of wavenumber-1 and wavenumber-2. Taking the idea of an improved topographic distribution was brought to its logical conclusion in Boyer and Chen (1987), where one mountain range in particular, in this case the Rocky Mountains, was modelled in great detail for a laboratory experiment. Conversely, however, this paper was criticised for bringing *too much* complexity to such a simple simulation of the atmosphere. James (1988), for example, noted that having such a detailed topography was of dubious worth when the walls of the annulus will produce reflection patterns that simply do not exist in the flow over the Rocky Mountains. From this, the lesson learnt is that less-idealised topography should not be a hyper-realistic reproduction of a planet's surface. Instead, a smaller change to basic sine wave topography is needed, to reflect the limitations of the physical annulus model. As such, the original idea of Li, Kung and Pfeffer (1986) can be revisited: using a superposition of wavenumbers to create a less-idealised distribution.

Hence, the subject of this thesis will be an investigation into the various superpositions of the first three wavenumbers. For example, the Fourier decomposition of the Southern Hemisphere of Mars, from Hollingsworth and Barnes (1996), suggests that its topography is formed from both a wavenumber-1 and a wavenumber-3. This is illustrated in Figure 5.5. The proposed study is therefore to carry out experiments with both of these types of topography separately (or just the wavenumber-3 type, if time does not permit both) at known points in parameter space, and then investigate a topography formed from their superposition under the same conditions. Not only will this highlight the effects of combining wavenumbers but it should furthermore give a reasonably accurate model for the Southern Hemisphere of Mars. In addition, the results of experiments under less-idealised topography may also go some way to answering the open questions of the previous section, confirming or denying the existence of multiple equilibria and determining the mechanism of formation for LFV, for example.

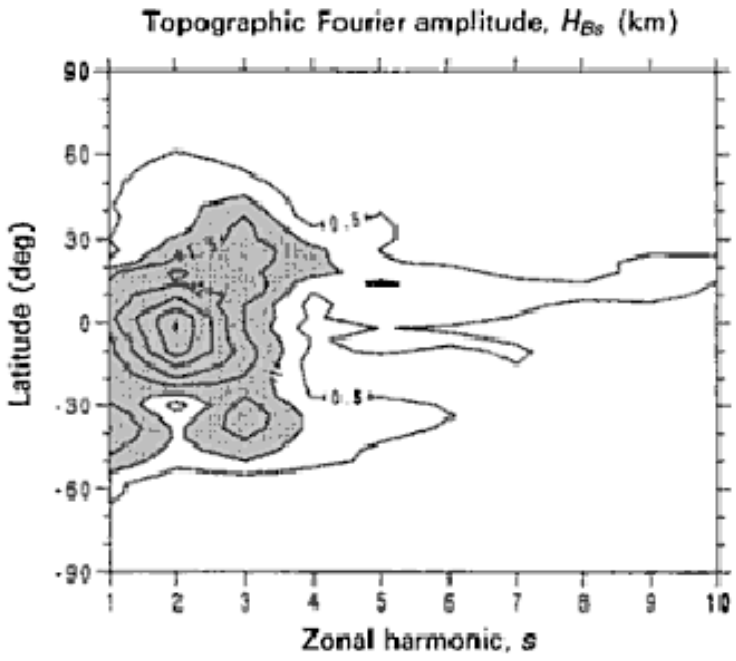

Figure 5.5: Fourier decomposition of Martian topography [from Read and Lewis (2004), created using a dataset by Hollingsworth and Barnes (1996)]

5.3 Modifications to Apparatus

Chapter 2 explained how the equipment was returned to the state that it had been in during use by the previous owner. However, a number of improvements presented themselves, and several new pieces of equipment were decided on. The three major additions are listed below:

- **Optiplex 780 USFF** – A Mini PC, similar to the Mac Mini (but with a Windows OS), chosen be attached to the superstructure in the rotating frame. In the same way that the Mac Mini is in charge of the camera functions, the Optiplex will control the Eurotherm via a serial port, as well as acquisition of thermocouple data.

- **USB TC-O8 Thermocouple Data Logger** – This device allows for thermocouple data acquisition. The annulus already has a number of thermocouples attached to its inner and outer walls, but the data logger provides a cold junction, in addition to necessary signal amplification of the data. It will be connected to the Optiplex using a USB slot.

- **Dell 780 MT 2.66 GHz Core Quad** – A faster and more powerful version of the current base station, intended to serve as its replacement. The current LAN will be extended to cover all the new hardware, allowing full wireless control of the Mac Mini and Optiplex from this computer.

With these new pieces of equipment, the camera will cease to be the sole source of data and the fluid temperature field can also be observed and studied. Despite the thermocouples being only attached to the inner and walls, and not protruding into the flow itself (which would cause unavoidable interference, as found by Leach (1981) and Hignett at el (1985), for example), the information gathered should provide greater detail of the baroclinic structure of the fluid and act as a comparison to the camera's flow velocity data for the study of topography. Such an arrangement was employed by Pfeffer, Kung and Li (1988) for their similar work to good effect. This temperature data will also be invaluable in the investigation of thermal boundary layers, if the study of inertia-gravity waves is resumed. An existing LabVIEW control system will be also adapted for future experiments, allowing manipulation of the rotation rates and temperature differences from a single program on the new base station (as well as ensuring that they are continuous).

A secondary purpose for the experiments of the first year was to ascertain the condition and working order of the apparatus. Whilst the various leaks of the heating and cooling systems had no practical impact on the investigation, and therefore could safely be ignored, the lighting array was found to be far more problematic. At some point prior to the beginning of this thesis the metal of the array had seemingly deformed, causing the lights to no longer exactly match up with their respective slits in the annulus. As such, the illumination was below optimal, especially at lower levels. Whilst this issue could be fixed, it seems prudent to replace the array of lamps with one of Ultra-Bright LEDs. Not only would this fix the illumination problem, but the light would be more focussed and less susceptible to picking up particles outside of its level. In addition, the three electric fans could be removed, reducing weight and clutter on the rotating frame.

Chapter 6

Further Work and Timeline

This chapter will summarise all the tasks planned for the next two years of this thesis. Firstly, the experiments devised in the last section of Chapter 4 to improve the bifurcation and inertia-gravity wave studies will be condensed. After that, the proposed topographic study of Chapter 5 will be broken into individual tasks. In the next section, a planned numerical study to complement the laboratory work will be discussed and its importance explained. Finally, a timeline is provided to illustrate when all of these tasks are planned to take place in the course of the thesis.

6.1 Further Work – First Year Studies

There are essentially four extensions to the studies conducted in this report. The first extension, for the bifurcation study, is to either replace the current annulus with a smaller version, as shown in Figure 2.7, or to construct a thermocouple array that can take temperature data across the entire flow profile. Whichever solution is chosen, the experiments will be performed in the same way as before – this time closer to the location of the bifurcation sequence. The second extension, also for the bifurcation study, is to continue to use the same annulus to examine the same area in parameter space as the Low Taylor Number experiments, with the aim of investigating further spatial period-doubling events. The third extension, for the inertia-gravity wave study, is to build an improved arrangement of equipment, with superior lighting sources and injection methods. The fourth extension, also for the inertia-gravity wave study, is to carry out more experiments over a greater number of points in parameter space, optimally with continuous control over rotation rates and temperature differences.

The two preliminary studies would then be able to develop into six new investigations:

- A repeat of the bifurcation study with a standard annulus or an extensive thermocouple array.
- A development of the bifurcation study with the goal of finding spatial period-doubling.
- An investigation into the limits of parameter space for where inertia-gravity waves occur.
- A comparison of instability rolls in water and water-glycerol mixture.
- A search for multiple instability rolls under any conditions.
- An examination of the effects of adding a rigid lid on the thermal boundary layer.

6.2 Further Work - Topography

As explained in Chapter 5, the major focus of the subsequent years of this thesis will be based upon improving the laboratory representation of topography by making it less idealised, the impact of this improvement on atmospheric circulation and whether the result creates a more appropriate topography for use in other laboratory and numerical experiments, as well as weather prediction models. Topography will be designed as a superposition of wavenumbers, based on Hollingsworth and Barnes' (1996) description of the Southern Hemisphere of Mars, to observe the effects of this superposition against simple wavenumber topography.

The opening task of the topographic study is to re-design the apparatus. Adding the Dell 780 MT 2.66 GHz Core Quad, the Optiplex 780 USFF and the USB TC-O8 Thermocouple Data Logger, as well as setting up a LabVIEW control system, will allow thermocouple data to be received and continuous remote manipulation over the rotation rates and temperature differences from the base station to be achieved. In addition, the lighting array requires replacing with one comprising of Ultra-Bright LEDs. At the same time, the three different topographic bases – wavenumber-1, wavenumber-3 and the superposition of the two – will be designed and sent off to be built. If the construction of the topography takes longer than expected, the wavenumber-1 base will be abandoned, and the investigation will solely focus on the other two.

The topography will be designed so that the peaks and troughs are large enough to begin to invalidate quasi-geostrophic theory, as explained in the next section. The topography will also include a 22° radial slope downwards from the inner wall to the outer wall. The slope simulates the beta effect of the atmosphere, which is otherwise ignored. This particular gradient was chosen due to the work of Wordsworth (2008), who created a similarly sloping Perspex lid (also necessary for the beta effect), carefully designing it so no optical properties were lost.

The experiments will first be carried out with the wavenumber-3 base, noting the differences to the flat-bottomed bifurcation study and determining locations of parameter space that provide repeatable, well-defined wave structures. The topography will then be replaced by the wavenumber-1 and the superposition bases, observing the differences to the flow under the same conditions. In this way, the investigation of superposition topography will begin, allowing for the possibility of further studies and extensions as progress is made. The objective of these further studies will be to find solutions to the open questions posed in Chapter 5, such as the growth-rate and time-scale of the various topographically forced oscillations and perturbations, the existence of multiple equilibria with less-idealised topography and the mechanism of generation of LFV. The apparatus could even be adapted further, for example by varying the long-term temperature difference to allow the seasonal

variation experiment suggested by Risch (1999), or by the addition of topographic 'blocks' to permit comparison to ocean circulation.

6.3 Numerical Study

QUAGMIRE, standing for *QUAsi-Geostrophic Model for Investigating Rotating fluids Experiments*, is different to those numerical models most commonly used in the literature (as mentioned in Chapter 5), as it is not employed to search for new atmospheric phenomena, but instead to increase the understanding of those already found. As the name suggests, it attempts to achieve this by having its geometry in the form of a rotating annulus like those used in laboratory. Unlike the otherwise similar MORALS (*Met Office/Oxford Rotating Annulus Laboratory Simulation*, see Farnell and Plumb (1975) for a full description), instead of challenging the full Navier-Strokes Equations and the many other equations that describe a flow, QUAGMIRE only solves the quasi-geostrophic potential vorticity equation. Williams, Read and Haine (2010) explained that, due to their simplicity and thus their ease of modelling, laboratory flows are excellent for studying "fundamental dynamical phenomena". However, the authors believed that models that solve the Navier-Strokes Equations are too computationally expensive to use for a large enough sample of flows. QUAGMIRE is the solution to this problem, with its greatly reduced computational expense. The model is also multi-layer, allowing the vertical structure of the atmosphere to be investigated as rigorously or as roughly as required[10]. On the other hand, the use of the quasi-geostrophic approximation means that no ageostrophic features of the flow can be simulated. The most notable absence is the boundary layers, which in turn means no Ekman Layers can exist. The remedy for this is to set boundary conditions via Ekman Pumping, but ageostrophic features will still not be modelled.

The reasoning behind using QUAGMIRE is twofold: firstly, as Hignett et al (1985) noted, an additional numerical study can greatly improve the accuracy of a laboratory study. The numerical model QUAGMIRE, already set up to simulate a differentially-heated annulus, will be employed for the same topographies, allowing comparison between the experimental and computational studies. The results gathered from these experiments will be contrasted, highlighting and removing as many errors as possible and hence reducing the risk of nonsense readings from either source.

[10] One- and two-layer models have already been discussed and, for example, Kondrashov, Ide and Ghil (2004) achieved a 'realistic' global simulation using a three-layer model.

Secondly, and most importantly, QUAGMIRE is a quasi-geostrophic model. Comparing its results to those from the physical annulus will test the limits of quasi-geostrophic theory. The theory is known to begin to break down at roughly the point where the ratio of the height of the topography to the height of the annulus becomes greater than or equal to the Rossby Number of the flow. This is what occurs in the atmosphere, if the height of the annulus is replaced by the height of the tropopause. As such, the magnitude of the topography designed, as well as the flow parameters used, will be chosen in such a way that this condition is met. The comparisons between the experiments will therefore show how well a quasi-geostrophic model copes in an ageostrophic environment and which ageostrophic aspects of sloped convection, if any, can be imitated. In addition, any flow features observed in the laboratory study, but not the numerical study, can be assumed to be ageostrophic in nature.

6.4 Timetable

Figure 6.1 shows an estimated timeline of this project, running from the current time until its end in the summer of 2012. The length of time allotted to each task is intentionally generous, to take into account the various potential delays for those assignments (such as long delivery times for parts). Hopefully, this will also mitigate the effect of any unforeseeable problems encountered (such as equipment failure or illness). As topography is the main focus of the second and third year of this thesis, the further studies into bifurcations and inertia-gravity waves will not be explicitly factored into the planned timeline. The penultimate task, however, is amongst the longest, allowing ample scope for further studies and experiments to be carried out, if the project does not fall behind schedule.

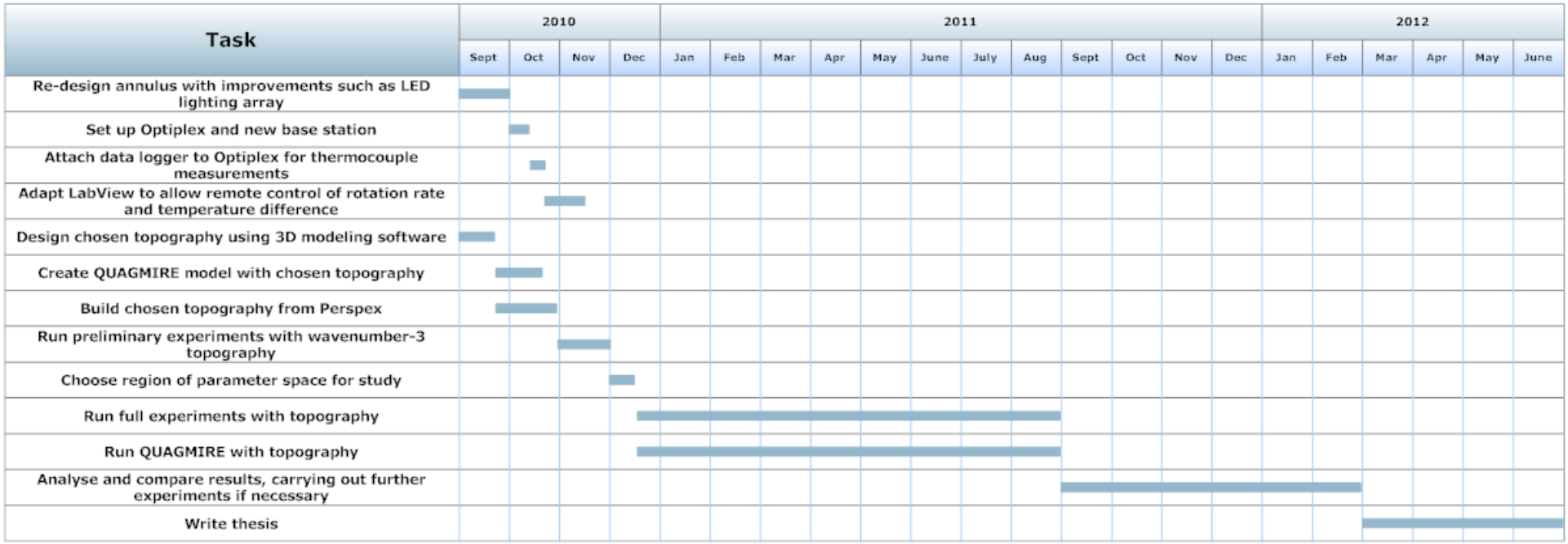

Figure 6.1: Proposed timeline for thesis

Chapter 7

References

Andrews, D.G., 2000. *An Introduction to Atmospheric Physics*. Cambridge: Cambridge University Press.

Benzi, R., Malguzzi, P., Speranza, A. & Sutera, A., 1986. The Statistical Properties of General Atmospheric Circulation: Observational Evidence and a Minimal Theory of Bimodality. *Quarterly Journal of the Royal Meteorological Society*, 112(473), pp.661-674.

Bernardet, P., Butet, A., Déqué, M., Ghil, M. & Pfeffer, R.L, 1990. Low Frequency Oscillations in a Rotating Annulus with Topography. *J. Atmos. Sci.*, 47(24), pp.3023-3043.

Boyer, D.L. & Chen. R., 1987. Laboratory Simulations of Mechanical Effects of Mountains on the General Circulation of the Northern Hemisphere: Uniform Shear Background Flow. *J. Atmos. Sci.*, 44(23), pp.3552-3575.

Cehelsky, P. & Tung, K.K., 1987. Theories of Multiple Equilibria and Weather Regimes – A Critical Reexamination. Part II: Baroclinic Two-Layer Models. *J. Atmos. Sci.*, 44(21), pp.3282-3303.

Charney, J.G. & DeVore, J.G., 1979. Multiple Flow Equilibria in the Atmosphere and Blocking. *J. Atmos. Sci.*, 36(7), pp.1205-1216.

Charney, J.G. & Straus, D.M., 1980. Form-Drag Instability, Multiple Equilibria and Propagating Planetary Waves in Baroclinic, Orographically Forced, Planetary Wave Systems. *J. Atmos. Sci.*, 37(6), pp.1157-1176.

Charney, J.G., Shukla, J. & Mo, K.C., 1981. Comparison of a Barotropic Blocking Theory with Observation. *J. Atmos. Sci.*, 38(4), pp.762-779.

Chomaz, J.M., Rabaud, M., Basdevant, C. & Couder, Y., 1988. Experimental and Numerical Investigation of a Forced Circular Shear Layer. *J. Fluid Mech.*, **187**, pp.115-140.

Farnell, L. & Plumb, R.A., 1975. Numerical Integration of Flow in a Rotating Annulus I: Axisymmetric Model. *Occasional Note Met O*, 21 75/3. [Unpublished Technical Report]

Fein, J.S. & Pfeffer, R.L., 1976. An Experimental Study of the Effects of the Prandtl Number on Thermal Convection in a Rotating, Differentially Heated Cylindrical Annulus of Fluid. *J. Fluid Mech.*, 75(1), pp.81-112.

Ghil, M. & Robertson, A.W., 2002. "Waves" vs. "Particles" in the Atmosphere's Phase Space: A Pathway to Long-Range Forecasting? *Proceedings of the National Academy of Sciences of the United States of America*, 99(1), pp.2493-2500.

Gollub, J.P. & Benson, S.V., 1980. Many Routes to Turbulent Convection. *J. Fluid Mech.*, 100(3), pp.449-470.

Hart, J.E., 1985. A Laboratory Study of Baroclinic Chaos on the f-Plane. *Tellus A*, 37A(3), pp.286-296.

Held, I.M., 1983. Stationary and Quasi-Stationary Eddies in the Extratropical Troposphere: Theory. In Hoskins, B.J. & Pearce, R.P., ed., *Large-Scale Dynamical Processes in the Atmosphere*. London: Academic Press Inc. (London) Ltd. Ch. 6.

Hide, R., 1953. Some Experiments on Thermal Convection in a Rotating Liquid. *Quarterly Journal of the Royal Meteorological Society*, 79(339), pp.161. [Correspondence]

Hide, R., 1958. An Experimental Study of Thermal Convection in a Rotating Liquid. *Philosophical Transactions of the Royal Society of London. Series A, Mathematical and Physical Sciences*, 250(983), pp.441-478.

Hide, R., Lewis, S.R. & Read, P.L., 1994. Sloping Convection: A Paradigm for Large-Scale Waves and Eddies in Planetary Atmospheres? *Chaos*, 4(2), pp.135-162.

Hide, R. & Mason, P.J., 1975. Sloping Convection in a Rotating Fluid. *Advances in Physics*, 24(1), pp.47-100.

Hignett, P., White, A.A., Carter, R.D., Jackson, W.D.N. & Small, R.M., 1985. A Comparison of Laboratory Measurements and Numerical Simulations of Baroclinic Wave Flows in a Rotating Cylindrical Annulus. *Quarterly Journal of the Royal Meteorological Society*, 111(463), pp.131-154.

Hollingsworth, J.L. & Barnes, J.R., 1996. Forced Stationary Planetary Waves in Mars's Winter Atmosphere. *J. Atmos. Sci.*, 53(3), pp.428-448.

Houghton, J., 2002. *The Physics of Atmospheres*. 3rd ed. Cambridge: Cambridge University Press.

Jacoby, T.N.L., Read, P.L., Williams, P.D. & Young, R.M.B., 2010. Generation of Inertia-Gravity Waves in the Rotating Thermal Annulus by a Localised Boundary Layer Instability. [Unpublished]

James, I.N., 1988. Meteorology of a Flat Earth. *Nature*, **333**, pp.118.

Jonas, P.R., 1981. Laboratory Observations of the Effects of Topography on Baroclinic Instability. *Quarterly Journal of the Royal Meteorological Society*, 107(454), pp.775-792.

Keppenne, C.L., 1992. Orographically Forced Oscillations in a Dynamical Model of the Martian Atmosphere. *Icarus*, 100(2), pp.598-607.

Keppenne, C.L. & Ingersoll, A.P., 1995. High-Frequency Orographically Forced Variability in a Single-Layer Model of the Martian Atmosphere. *J. Atmos. Sci.*, 52(11), pp.1949-1958.

Kondrashov, D., Ide, K. & Ghil, M., 2004. Weather Regimes and Preferred Transition Paths in a Three-Layer Quasigeostrophic Model. *J. Atmos. Sci.*, 61(5), pp.568-587.

Knox, J.A., McCann, D.W. & Williams, P.D., 2008. Application of the Lighthill-Ford Theory of Spontaneous Imbalance to Clear-Air Turbulence Forecasting. *J. Atmos. Sci.*, 65(10), pp.3292-3304.

Koo, S. & Ghil, M., 2002. Successive Bifurcations in a Simple Model of Atmospheric Zonal-Flow Vacillation. *Chaos*, 12(2), pp.300-309.

Leach, H., 1981. Thermal Convection in a Rotating Fluid: Effects due to Bottom Topography. *J. Fluid Mech.*, **109**, pp.75-87.

Li, Q.G., Kung, R. & Pfeffer, R.L., 1986. An Experimental Study of Baroclinic Flows with and without Two-Wave Bottom Topography. *J. Atmos. Sci.*, 43(22), pp.2585-2599.

Molteni, F., 1996. On the Dynamics of Planetary Flow Regimes, Part II: Results from a Hierarchy of Orographically Forced Models. *J. Atmos. Sci.*, 53(14), pp.1972-1992.

Pfeffer, R.L., Kung, R. & Li, Q.G., 1988. Some Effects of Rotation Rate on Planetary-Scale Wave Flows. *Theoretical and Applied Climatology*, 55(1-4), pp.199-210.

Rabaud, M. & Couder, Y., 1983. A Shear-Flow Instability in a Circular Geometry. *J. Fluid Mech.*, **136**, pp.291-319.

Randriamampianina, A., private communication. [Conversation – 30/07/2010]

Randriamampianina, A., Früh, W.G., Read, P.L. & Maubert, P., 2006. Direct Numerical Simulations of Bifurcations in an Air-Filled Rotating Baroclinic Annulus. *J. Fluid Mech.*, **561**, pp.359-389.

Read, P.L. & Lewis, S.R., 2004. *The Martian Atmosphere Revisited: Atmosphere and Environment of a Desert Planet*. Chichester: Praxis Publishing Ltd.

Reinhold, B.B. & Pierrehumbert, R.T., 1982. Dynamics of Weather Regimes: Quasi-Stationary Waves and Blocking. *Mon. Wea. Rev.*, 110(9), pp.1105-1145.

Risch, S.H., 1999. *Large-Scale Wave Interactions in Baroclinic Flow with Topography*. DPhil. University of Oxford.

Tian, Y., Weeks, E.R., Ide, K., Urbach, J.S., Baroud, C.N., Ghil, M. & Swinney, H.L., 2001. Experimental and Numerical Studies of an Eastward Jet over Topography. *J. Fluid Mech.*, **438**, pp.129-157.

Tung, K.K. & Rosenthal, A.J., 1985. Theories of Multiple Equilibria and Weather Regimes – A Critical Reexamination. Part I: Barotropic Models. *J. Atmos. Sci.*, 42(24), pp.2804-2819.

Vettin, F., 1857. Ueber den aufsteigenden luftstrom, die entstehung des hagels und der wirbel-stuerme. *Annalen der Physik*, 178(10), pp.246-255.

Völker, C., 1999. Momentum Balance in Zonal Flows and Resonance of Baroclinic Rossby Waves. *J. Phys. Oceanogr.*, 29(8), pp.1666-1681.

Wallace, J.M., 1983. The Climatological Mean Stationary Waves: Observational Evidence. In Hoskins, B.J. & Pearce, R.P., ed., *Large-Scale Dynamical Processes in the Atmosphere*. London: Academic Press Inc. (London) Ltd. Ch. 2.

Williams, G.P., 1967. Thermal Convection in a Rotating Fluid Annulus: Part 2. Classes of Axisymmetric Flow. *J. Atmos. Sci.*, 24(2), pp.162-174.

Williams, P.D., Read, P.L. & Haine, T.W.N., 2003. Spontaneous Generation and Impact of Inertia-Gravity Waves in a Stratified, Two-Layer Shear Flow. *Geophys. Res. Lett.*, 30(24), pp.2255-2258.

Williams, P.D., Read, P.L. & Haine, T.W.N., 2010. Testing the Limits of Quasi-Geostrophic Theory: Application to Observed Laboratory Flows Outside of the Quasi-Geostrophic Regime. *J. Fluid Mech.*, **649**, pp.187-203.

White, F.M., 2008. *Fluid Mechanics*. 6th ed. New York: McGraw-Hill.

Wordsworth, R.D., 2008. *Theoretical and Experimental Investigations of Turbulent Jet Formation in Planetary Fluid Dynamics.* DPhil. University of Oxford.

Yang, S., Reinhold, B. & Källén, E., 1997. Multiple Weather Regimes and Baroclinically Forced Spherical Resonance. *J. Atmos. Sci.*, 54(11), pp.1397-1409.

Young, R.M.B. & Read, P.L., 2008. Flow transitions resembling bifurcations of the logistic map in simulations of the baroclinic rotating annulus. *Physica D*, 237(18), pp.2251-2262.